# Characterisation of Zein Microcapsules with Encapsulated Geraniol or Wintergreen Essential Oil for Controlled Release as an Aphid Repellent

Ignatius Van Wyk Ferreira

Submitted in partial fulfilment of the requirements for the degree Master of Engineering (Chemical Engineering)

Department of Chemical Engineering

Faculty of Engineering, Built Environment and Information Technology,
University of Pretoria, Pretoria, South Africa

2016

UNIVERSITEIT VAN PRETORIA
UNIVERSITY OF PRETORIA
YUNIBESITHI YA PRETORIA

CVD 800

# Characterisation of Zein Microcapsules with Encapsulated Geraniol or Wintergreen Essential Oil for Controlled Release as an Aphid Repellent

By: Ignatius Van Wyk Ferreira

Supervisor: Prof. Walter Wilhelm Focke

Department: Chemical Engineering

Degree: MEng (Chemical Engineering)

## Synopsis

Microencapsulation of geraniol and wintergreen oil by the maize protein, zein, was investigated. The efficiency of encapsulation, the morphology of micro-particles and the controlled-release kinetics of the geraniol-zein system were studied.

The main findings were the following:

- Geraniol-to-zein mass ratios lower than unity showed very low particle yields. At ratios higher than unity an abrupt increase in particle yield was observed. It reached values as high as 85%. Concurrently high geraniol mass fractions up to 78% were realised. This unusual behaviour is proposed to be attributed either to the inversion of the zein globular structure driven by an increase in the hydrophobicity of the surrounding medium or to the increased phase separation kinetics of the geraniol.
- Insignificant particle yields for the wintergreen oil-zein system may be attributed to the high polarity of methyl salicylate.
- Geraniol and wintergreen oil-containing micro-particles had a spherical geometry prior to lyophilisation.

- Scanning electron and confocal microscopy revealed that the geraniol-zein micro-particles can be classified as reservoir systems. Release kinetics approaching zero-order release, consistent with a glassy reservoir system, were observed.
- Kinetic modelling predicts that 80% of encapsulated geraniol can be released over a period of 17 days at 20 ˚C.
- The results mean that the geraniol-zein microcapsule system holds promise and that it should be possible to produce it for large-scale, sustainable agricultural use as an aphid repellent.

It is recommended that the release kinetics of the geraniol-zein system be studied in an aqueous environment and that other polar biopolymers be investigated.

Keywords: micro-encapsulation; zein; geraniol; wintergreen oil; controlled release; aphid

# Acknowledgements

I would like to express my gratitude to my supervisor, Prof. Walter W. Focke, for his continuous support and excellent guidance. It has been a great honour for me to work with such a remarkable person, remarkable in both his professional and personal capacity.

Furthermore, I would like to thank Ms. Elizbe L. du Toit for her assistance with some of the experimental work and her motivation.

A special thanks to Ms. Sandra Wyngaardt and Prof. Jan A. Verschoor from the Department of Biochemistry for making their freeze drier available for my use and Sandra's willingness to assist me with the utmost kindness.

Thanks to all the personnel of the University of Pretoria, especially the Institute of Applied Materials, for their friendliness and help.

Lastly, thanks to my family, especially my parents, for their lifelong support, motivation and more love than I think I deserve. You are more than I could ever have asked for.

# Table of Contents

# List of Figures

# List of Tables

# Nomenclature

| | | |
|---|---|---|
| $A_k$, B , C | Antoine constants | [-] |
| *a* | Radius of molecule | [µm] |
| Aij, Aji | Margules constants | [-] |
| *A* | Area | [$m^2$] |
| *c* | Concentration of release substance | [$kg/m^3$] |
| *D* | Diffusivity | [$m^2/s$] |
| *d* | Diameter of microcapsule | [m] |
| De | Deborah number | [-] |
| $E_a$ | Activation energy | [J/mol] |
| *j* | Mass flux | [$kg/(m^2\ s)$] |
| *k* | Release constant | [1/min] |
| $k_B$ | Boltzmann's constant | [J/K] |
| $m_{AV}$ | Mass of volatile added | [mg] |
| $m_{AZ}$ | Mass of zein added | [mg] |
| $m_D$ | Mass of dried microcapsules | [mg] |
| $m_{EV}$ | Mass of encapsulated volatile | [mg] |
| $m_o$ | Mass of volatile released at infinity | [mg] |
| $m_{PV}$ | Mass of volatile that participated in encapsulation | [mg] |
| $m_{PZ}$ | Mass of zein that participated in encapsulation | [mg] |
| $m_r$ | Mass of volatile released | [mg] |
| $m_t$ | Mass of volatile remaining at time *t* | [mg] |
| $m_T$ | Total mass of zein and geraniol added | [mg] |
| $m_{TM}$ | Total mass of microcapsules | [mg] |
| n | Release exponent constant | [-] |

| | | |
|---|---|---|
| $P_i$ | Vapour pressure of substance *i* | [kPa, mmHg] |
| R | Universal gas constant | [J/(mol K)] |
| $T$ | Temperature | [˚C, K] |
| $t$ | Time | [s, min] |
| $x$ | Wall membrane thickness | [µm,m] |
| $x_i$ | Liquid mole fraction of *i* volatile | [-] |
| $y_i$ | Vapour mole fraction of *i* volatile | [-] |
| $w_i$ | Liquid mass fraction of component *i* | [-] |
| | | |
| $\gamma_i$ | Activity coefficient of substance *i* | [-] |
| $\mu$ | Dynamic viscosity | [Pa·s] |
| $\vartheta$ | Solvent diffusion time | [s] |
| $\xi$ | Geraniol to zein mass ratio | [-] |
| $\rho_i$ | Density of substance *i* | [kg/m$^3$] |
| $\tau$ | Polymer relaxation time | [s] |

# 1 Introduction

Aphids are destructive pests of economically important crops throughout the world. They damage the plants by imbibing sap causing wilting of the plant, injection of toxic saliva and the production of honeydew (Blackman, 1974). In addition, aphids transmit more plant viruses than any other sap-feeding insects (Dewhirst et al., 2010). The accompanying environmental problems caused by the overuse of current pesticides have become a concern in recent years. An alternative to the use of pesticides is essential oils with insect repellent properties which cause fewer concerns about animal and environmental toxicity (Koul et al., 2008).

However, due to the volatility of essential oils, the sustained release thereof for pest management remains a challenge (Allsopp et al., 2014). Applied in emulsion form, essential oils require relatively high application rates and will also require frequent re-application, which renders their use for large-scale agricultural applications both unpractical and uneconomical. A well-known solution is to micro-encapsulate the volatile in a polymer shell to control its release (Brinkhuis et al., 2011).

The objective of this study was to determine whether geraniol, a major constituent of lemon grass essential oil (Ricci et al., 2006) and wintergreen oil, the essential oil of the evergreen Wintergreen shrub (*Gaultheria procumbens*), could be micro-encapsulated by the biodegradable corn protein, zein. Geraniol and the major constituent of wintergreen oil, methyl salicylate, are proven aphid repellents (Halbert et al., 2008, Hardie et al., 1994), while zein is a protein by-product yet to be used as an industrial polymer (Shukla and Cheryan, 2001). Subsequent objectives were to gain insight into the mechanism of micro-encapsulation and to characterise the efficiency of the micro-encapsulation at different volatile-to-zein mass ratios, the microcapsule geometry and structure, and the release kinetics of the micro-encapsulated volatiles. The ultimate goal is to utilise the volatile-containing microcapsules in agricultural irrigation systems for pest control.

The geraniol and wintergreen oil were dispersed in an ethanol-water solution containing zein, after which the phase separation technique was used to form the microcapsules.

Phase separation occurred upon the addition of additional water. The resultant micro-particles were lyophilised for characterisation purposes.

# 2 Theoretical Background

## 2.1 Zein

There are four primary methods by which corn is processed, namely dry milling, alkaline processing, wet milling and the dry-grind process. The products of the dry-milled and alkaline-processed corn are for direct human consumption (Watson and Ramstad, 1987). Of the two remaining processes, the primary use of corn in the dry-grind process is for the production of ethanol, which renders protein by-products contained in distillers dried grains (DDG) and DDG with solubles (DDGS). The main products of the wet milling process are starch and oil and it also renders protein by-products known as corn gluten meal (CGM) and corn gluten feed (CGF). The CGM is the main concern, as this is where the endosperm proteins of a corn kernel are mostly found.

Zein is a corn protein that belongs to the characteristic class of proteins known as prolamines, which are high in proline and glutamine amino acid content. It is almost entirely present in the endosperm of a corn kernel, which constitutes 75% of protein present in a corn kernel (overall 6–12% of a corn kernel consists of protein). These by-products are currently incorporated into animal feed. However, zein is deficient in essential amino acids, such as lysine and tryptophan, and yields poor nutritional value. It is insoluble in water and this limits its use in food products. Therefore there has been an effort to utilise zein as an industrial polymer since the mid-20th century (Shukla and Cheryan, 2001).

### 2.1.1 Composition

The solubility behaviour of zein can be explained by its amino acid composition, of which a great proportion consists of non-polar amino acids with low fractions of basic and acidic amino acids. This can be seen in Table 2-1, which shows the amino acid composition of commercial zein.

It is clear that zein is constituted of a variety of amino acids that can be categorised into classes with differing properties, which is why zein is regarded as an amphiphilic substance (Kim and Xu, 2008). The majority of the amino acids are, however, nonpolar at 53.4%,

which explains the overall hydrophobic behaviour of zein. These different amino acid classes are not homogeneously present in the zein structure as zein is comprised of a mixture of different polypeptides, with differing compositions of amino acids resulting in a range of molecular sizes, solubility and charges.

**Table 2-1: Amino acid composition of zein (Pomes, 1971).**

| **Amino acid** | **Class** | **Mass fraction** (%) |
|---|---|---|
| Glycine | Nonpolar | 0.7 |
| Alanine | Nonpolar | 8.3 |
| Valine | Nonpolar | 3.1 |
| Leucine | Nonpolar | 19.3 |
| Isoleucine | Nonpolar | 6.2 |
| Phenylalanine | Nonpolar | 6.8 |
| Tryptophane | Nonpolar | NR |
| Proline | Nonpolar | 9.0 |
| Serine | -OH | 5.7 |
| Threonine | -OH | 2.7 |
| Tyrosine | -OH | 5.1 |
| Methionine | -S | 2.0 |
| Cysteine | -S | 0.8 |
| Lysine | Basic | NR |
| Arginine | Basic | 1.8 |
| Histidine | Basic | 1.1 |
| Aspartic acid | Acidic | NR |
| (as aspargine) | Acidic | 4.5 |
| Glutamic acid | Acidic | 1.5 |
| (as glutamine) | Acidic | 21.4 |

This leads to the fractionation of zein according to structures that shared common properties. The methods used to distinguish these fractions were precipitation (Watson et al., 1936), cation exchange chromatography (Craine et al., 1961), charcoal and gel filtration (Danzer et al., 1975), etc. which resulted in the definition of multiple fractions.

The fractionation of zein according to differential solubility provides the best understanding (Esen, 1986, Esen, 1987, Shukla and Cheryan, 2001). Zein can be categorised into fractions according to their solubility in isopropyl alcohol (IPA); namely α-zein, β-zein and γ-zein (Esen, 1986, Esen, 1987). The properties of these fractions are given in Table 2-2. It can be concluded from Table 2-2 that the properties of commercial zein will be close to those of α-zein as it forms the major fraction. α-Zein has large amounts of hydrophobic residues (Gianazza et al., 1977), hence its particular hydrophobic nature.

**Table 2-2: Properties of α-zein, β-zein and γ-zein fractions.**

| Zein fraction | Solubility characteristic | Mass fraction of zein (%) | Molecular weight of polypeptides (kD) |
|---|---|---|---|
| α-zein | Soluble in 50-95% IPA but insoluble in 30% IPA/30 mM Na-acetate | 75-85 | 21-25 and 10 |
| β-zein | Soluble in 30-95% IPA that contained a reducing agent but insoluble in 90% IPA (without a reducing agent) and 30% IPA/30 mM Na-acetate | 10-15 | 17-18 |
| γ-zein | Soluble in 0-80% IPA with a reducing agent and 30% IPA/ 30 mM Na-acetate | 5-10 | 27 |

### 2.1.2 Structure

It has been proposed that zein has a helical coil structure where nine homologous repeating units are arranged in an anti-parallel form stabilised by hydrogen bonds (Argos et al., 1982). It has been indicated that the helical content of zein varies between 33.6% and 60% in 50-80% ethanol (Argos et al., 1982, Danzer et al., 1975, Gortner and Macdonald, 1944, Matsushima et al., 1993). This suggests that zein has a globular structure in non-aqueous solutions (Danzer et al., 1975), also described as macromolecular micelles (Wang et al., 2004b, Wang et al., 2004a). An illustration of the proposed zein structure is given in Figure 2-1.

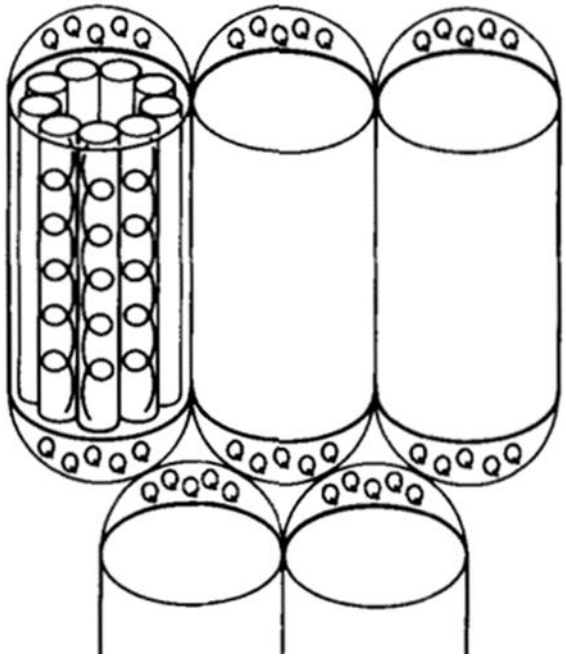

**Figure 2-1: Proposed helical wheel structure of the zein molecule (Argos et al., 1982).**

It is known that zein undergoes conformational changes as the ethanol content is varied from 50 - 80% (Shukla and Cheryan, 2001), although the behaviour of individual zein molecules is not known. However, it has been shown that the size of the macromolecular micelles decreases as the ethanol content is increased from 70 - 90% and then suddenly increases at ethanol concentrations higher than 90%. This was explained by the suggestion that a micellar inversion takes place depending on the nature of the solvent with regard to hydrophobicity and hydrophilicity (Wang et al., 2004b, Wang et al., 2004a).

### 2.1.3 Properties

One of the main properties of concern in this investigation is the solubility of zein. As established, zein is an amphiphilic amorphous powder, but due to its high content of nonpolar amino acids, it is insoluble in water (Shukla and Cheryan, 2001). An extensive list of non-aqueous solvents, mixtures of non-aqueous solvents and mixtures of non-aqueous solvents and water is available (Evans and Manley, 1941, Evans and Manley, 1944). Ethanol-water mixtures have been extensively used in the commercial production of zein (Shukla and Cheryan, 2001) and in experimental work with zein (Kim and Xu, 2008), and consequently an ethanol-water mixture was chosen for this investigation.

A phase diagram shows that the solubility of zein varies from 2 - 60% depending on the ethanol content (50 - 90%). Maximum solubility is achieved at approximately 60% ethanol content in the ethanol-water mixture. At ethanol concentrations lower than 40% and higher than 90% between the precipitation regions, a coacervation region exists where two liquid phases appear, both containing water, ethanol and zein (Mossé, 1961).

Other properties of importance of zein are its thermal degradation point at 320 ˚C, specific gravity of 1.25 at 25 ˚C (Shukla and Cheryan, 2001) and its biodegradability.

### 2.1.4 Zein as an encapsulating biopolymer

Zein has been investigated in numerous studies as an agent to encapsulate substances the release of which needs to be controlled. The major advantage of zein is its hydrophobic nature, which causes it not to undergo significant swelling (see Section 2.7) when in contact with water, but it still yields controlled release in an aqueous environment (Park et al., 1995, Wu, 1995). The substances encapsulated are medicinal drugs (Liu et al., 2005), fatty acids (Quispe-Condori et al., 2011), fertilisers, agents for environmental clean-up (Shukla and Cheryan, 2001) and pesticides (Redding, 1990).

## 2.2 Aphids

Aphids are small (1.5–3.5 mm), soft-bodied insects (Blackman and Eastop, 2000) that feed exclusively on sap from the vascular tissues of plants, mainly the phloem. Aphids are the main insect pests of agricultural crops in temperate regions, and they cause major economic losses (Dewhirst et al., 2010).

Aphids can damage plants by imbibing sap causing the plant to wilt, by injecting toxic saliva, and by producing honeydew (which encourages sooty moulds to colonise leaf surfaces and decreases photosynthesis in the plant)(Blackman, 1974). The even more damaging effect that aphids have on plants is their ability to transmit plant viruses due to their biology and feeding behaviour. Aphids transmit more plant viruses than any other sap-feeding insects (Dewhirst et al., 2010). Approximately 200 aphid species are known to transmit 275 viruses of 19 plant virus genera (Nault, 1997). Consequently, aphids are destructive pests of many economically important crops throughout the world (Fan et al., 2015). The major problem with controlling aphids is that they do not colonise affected crops, making insecticide treatment ineffective, and if repellents such as reflective mulch and whitewash paint are used, plants tend to overgrow the mulch and the paint inhibits photosynthesis.

## 2.3 Essential oils

### 2.3.1 Composition

Essential oils are volatile, natural, complex compounds characterised by a strong odour and are formed by aromatic plants as a secondary metabolite, i.e. they are an intermediate or product of metabolism that has an important ecological effect.

Essential oils can consist of 20 to 60 components, but are usually characterised by two or three major components. The major components determine the biological properties of essential oils (Bakkali et al., 2008). The components of essential oils can be categorised into two groups: the main group consists of terpenes and terpenoids, and the other group consists of aromatic components.

Terpenes are derived biosynthetically from isoprene $C_5H_8$, therefore the basic formulae for terpenes are multiples of isoprene $(C_5H_8)_n$, where n dictates the class of the terpene. Terpenes therefore usually contain one or more carbon-carbon double bonds (Hydrocarbons). The precursor to terpenes is isopentenyl diphosphate (IPP). More IPP's are then added which leads to the different classes of terpenes, and ultimately the allylic prenyl diphosphate undergoes specific synthetases to form the terpene skeleton with secondary enzymatic modification to give terpene its characteristic functional groups. Consequently terpenes can have varying structures (linear or ring) and different properties. Some of the terpene classes are hemiterpenes (n=1), monoterpenes (the most common, n=2) and diterpenes (n=4). Terpenoids are simply terpenes containing oxygen.

Aromatic compounds have a different biosynthetic pathway than that of terpenes and are derived from phenylpropane. The pathways for terpenes and aromatic compounds may coexist, but usually one becomes the major pathway (Bakkali et al., 2008).

### 2.3.2 Essential oils as a defence mechanism

Essential oils play an important role in the protection of plants as antibacterials, antivirals, antifungals and insecticides, and protect against herbivores. They are also useful in the attraction of desirable insects to aid in the dispersion of seeds and pollens, or they can repel undesirable insects (Bakkali et al., 2008). Plant volatiles (of which the terpenes are a major category among fatty acids) are normally released in small quantities. However, during the activity of herbivorous insects, they are released in much larger quantities, depending on the herbivorous insect attacking the plant. This release may also induce self-defence responses in neighbouring plants and act as semiochemicals (Paré and Tumlinson, 1999).

## 2.4 Geraniol

Geraniol is one of the major components found in various essential oils, e.g. ninde oil (66%) (Başer et al., 2005), rose oil (44.4%) (Baydar and Baydar, 2005), palmarosa oil (53.5%) (Dubey and Luthra, 2001) and citronella oil (24.8%) (Rajeswara Rao et al., 2004). It has a clear to pale yellow appearance and a characteristic rose-like odour (Chen and Viljoen, 2010), which is why it is commonly referred to as the poor man's rose oil and is widely used as a fragrance material. Geraniol falls under the major terpene/terpenoid group of essential oil components. It is an acyclic monoterpene alcohol and is therefore a terpenoid.

### 2.4.1 Structure

The IUPAC name for geraniol is 3,7-dimethylocta-trans-2,6-dien-1-ol. It must be noted that the commercial product referred to as geraniol is a mixture of two trans-cis isomers named geraniol (trans) and nerol (cis) (Chen and Viljoen, 2010). Both structures have the chemical formula $C_{10}H_{18}O$. The chemical structures of geraniol and nerol are given in Figure 2-2.

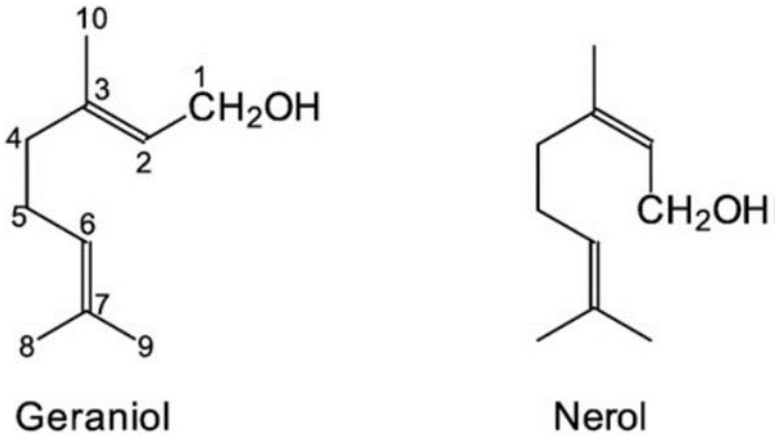


**Figure 2-2: Chemical structures of geraniol and nerol (Chen and Viljoen, 2010).**

### 2.4.2 Properties

The properties of geraniol are summarised in Table 2-3.

**Table 2-3: Chemical and physical properties of geraniol.**

| Description | Value |
|---|---|
| Molar mass (g/mol) | 154.25 |
| Solubility in water (g/L) | 0.1 (effectively insoluble) |
| Boiling point at 1 atm (˚C) | 230 |
| Auto-ignition temperature (˚C) | 250 |
| Density at 20 ˚C (g/mL) | 0.879 |
| Dipole moment (D) | 1.349 |

(Lide, 2004) (CID=637566 n.d.)

The vapour pressure data of geraniol are presented by the Antoine Equation given by Equation 1.

$$\log P(T) = A_k - B\,(T+C) \qquad (1)$$

where $P$ is the vapour pressure in (mmHg) and $T$ is the temperature in ˚C. The values of the constants $A_k$, B and C are 8.60515, 2773.11 and 254.443 respectively. The equation for geraniol is valid between the temperatures of 4 and 230 ˚C (Yaws et al., 2005).

According to the GPS Safety summary of BASF, geraniol is considered to be of low toxicity after single ingestion, virtually nontoxic after single skin contact and is also not considered toxic after repeated exposure. However, skin irritation and sensitisation are possible, and geraniol could cause severe damage to the eyes. Geraniol is considered not to be mutagenic or carcinogenic.

With regard to environmental impact, geraniol is considered to be readily biodegradable, and significant accumulation in organisms is not thought likely (GPS Safety Summary Geraniol).

### 2.4.3 Geraniol oil as an insecticide/insect repellent

Geraniol has been shown to be an effective acaricide (insecticide against mites and ticks). Its acaricidal activities against the storage food mite, *Tyrophagus putrescentiae*, were compared to those of benzyl benzoate and proved to be more effective (Jeon et al., 2009). Geraniol is also known to be an effective mosquito repellent (Omolo et al., 2004) in the form of commercially available candles. They have been found to be more effective than citronella and linalool candles (Müller et al., 2008).

Most importantly for this application, geraniol shows promise as an aphid repellent with reference to *Rhopalosiphum maidis* (Halbert et al., 2008)**,** and it has been concluded that lemongrass oil (of which the main constituents are geraniol, citral and myrcene) is effective in repelling the Russian Wheat Aphid, *Duraphis noxia* (Ricci et al., 2006).

## 2.5 Wintergreen oil

Wintergreen oil is an essential oil from the evergreen shrub Wintergreen (*Gaultheria procumbens*), which occurs in the eastern parts of North America. It is also known as Oil of Wintergreen or Gaultheria Oil. It has a pale yellow to pink appearance and has a distinctive fresh woody, medicinal odour and flavour (Gurung, 2007). It is used in many chewing gums, candles, toothpastes and mouthwashes (Facciola, 1998). The component responsible for this is methyl salicylate, which makes up approximately 96 - 98% of wintergreen oil (Gurung, 2007, Nikolić et al., 2013)

### 2.5.1 Structure

Methyl salicylate is an ester with the IUPAC name methyl 2-hydroxybenzoate and chemical formula $C_8H_8O_3$. The chemical structure of methyl salicylate is shown in Figure 2-3.

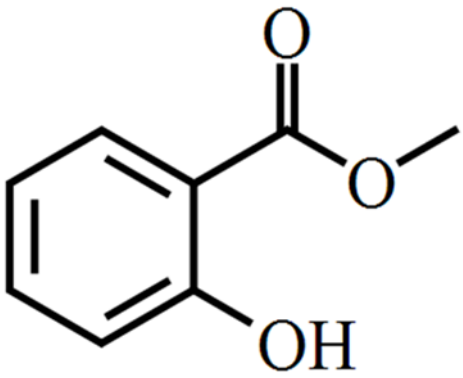


**Figure 2-3: Chemical structure of methyl salicylate (Lapczynski et al., 2007).**

### 2.5.2 Properties

The properties of methyl salicylate are given in Table 2-4.

**Table 2-4: Chemical and physical properties of methyl salicylate.**

| Description | Value |
|---|---|
| Molar mass (g/mol) | 152.15 |
| Solubility in water (g/L) | 1.875 (regarded as insoluble) |
| Boiling point at 1 atm (˚C) | 222 |
| Auto-ignition temperature (˚C) | 451 |
| Density at 20 ˚C (g/mL) | 1.18 |
| Dipole moment (D) | 2.47 |

(Lide, 2004) (CID=4133 n.d.)

### 2.5.3 Wintergreen oil as an insecticide/insect repellent

Methyl salicylate is well known as a herbivore-induced defence volatile, which is not only present in the Wintergreen shrub, but has also been detected in the head space of other insect-infested plants, e.g. soybean (Zhu and Park, 2005), tomato (Ament et al., 2004) and lima bean (Arimura et al., 2002).

Various studies have shown methyl salicylate to be an effective insect repellent, e.g. it repels the black bean aphid, *Aphis fabae* (Hardie et al., 1994), and the bird-cherry-oat aphid, *Rhopalosiphum padi L.* (Petersson et al., 1994). It should, however, be noted that the impact of aphid-repelling substances cannot be generalised as they affect various aphid species differently (Bernasconi et al., 1998).

## 2.6 Methods of encapsulation

### 2.6.1 Microfluidic method

The microfluidic approach can be used to create water-in-oil emulsions or oil-in-water emulsions by channelling the two immiscible fluids through a microfluidic device and mixing them. A schematic of such a device is shown in Figure 2-4.

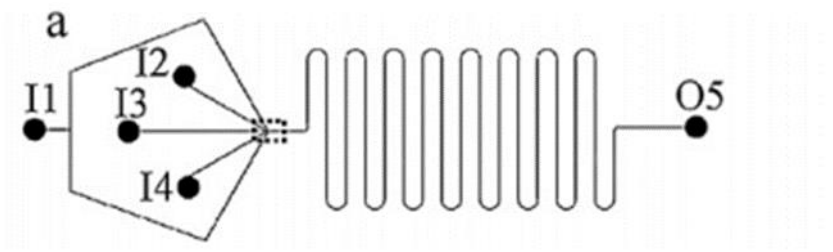


**Figure 2-4: Schematic of a microfluidic device (Fang and Cathala, 2010).**

Water-in-oil emulsions can be made by introducing the continuous oil phase through inlet 1 and introducing water, pectin (the polysaccharide used for encapsulation) and calcium chloride (the cross-linking agent of pectin) through inlets 3, 2 and 4 respectively. This enabled the individual production of pectin microcapsules (Fang and Cathala, 2010). The major advantage of this method is that the size of the microcapsule can be minutely controlled by simply adjusting the flow of the immiscible fluids through the channels (usually through controlling syringe pumps). This results in monodisperse microcapsules with almost 100% encapsulation (Okushima et al., 2004). Furthermore, it allows control over the shape, morphology and internal structure of the microcapsules through different microfluidic device geometries (Nie et al., 2005).

This method could possibly be applied to the geraniol-zein and wintergreen oil-zein systems in this study by dispersing the oil in water through two channels and introducing a zein-ethanol-water solution through a third channel, causing the zein to precipitate (the concentration of ethanol and water in the final solution can be controlled through manipulating the flow of the various compounds). This can be an extremely effective method, but the scalability of the method to produce large amounts of microcapsules for agricultural use is in doubt.

### 2.6.2 Supercritical anti-solvent method

This method is analogous to spray drying and enables the production of microcapsules by using supercritical carbon dioxide. The method requires the encapsulating polymer to be dissolved in a solvent or solvent mixture; typically for zein this will be an ethanol and water mixture. The solvent mixture has to be miscible with carbon dioxide as the carbon dioxide has to extract the solvent when the polymer solution is sprayed into it. The extraction causes the polymer concentration to increase and the ultimate precipitation of the polymer.

This method has been shown to be successful for the encapsulation of lysozyme with zein by dissolving the zein in a 90% ethanol water-ethanol mixture (Zhong et al., 2009). A possible method of applying this to the geraniol-zein and wintergreen-zein systems is to disperse the geraniol or the wintergreen in a zein-water-ethanol mixture and to inject the emulsion into the carbon dioxide.

The method is regarded as a promising scalable technique (Jung and Perrut, 2001), so industrial production may be possible. The only possible disadvantage of this method is the requirement of a pressure vessel; a pressure vessel was filled with carbon dioxide at 40 ˚C to 10 MPa for the encapsulation of lysozyme (Zhong et al., 2009). In addition, high-pressure pumps are required to feed the polymer solution and to purge the pressure vessel with carbon dioxide. These pieces of equipment will lead to increased costs and may pose a safety risk with legal requirements playing a role.

### 2.6.3 Phase separation method by mixing

This is, in my opinion, by far the simplest method to prepare zein microcapsules. It simply entails dispersing the substance to be encapsulated with a mixer in a solution that contains zein. Water is then abruptly added to the solution so that the ethanol concentration is lowered below the solubility range of zein i.e. typically to less than 40% ethanol. This causes the zein to precipitate out and, it is hoped, the dispersed substance will be encapsulated. This method was successfully employed to encapsulate ivermectin and flax oil with zein (Liu et al., 2005, Quispe-Condori et al., 2011). The simplicity and robustness of this method makes it very attractive. It is clearly scalable, and although there might be some mixing effects, it can likely be used to produce microcapsules on an industrial scale.

## 2.7 Controlled release characteristics

### 2.7.1 Mechanism of controlled release

All molecules undergo random collisions with other molecules, which leads to Brownian motion. The direction of the motion of the molecules caused by the collisions are random and changes constantly. However, macroscopically, the independent direction of the motions lead the molecules from a higher concentration to a lower concentration. This is termed as diffusion and is the mechanism by which an active substance is released from a polymeric micro-particle system.

The diffusivity of the molecule depends on the molecule itself and the medium through which it has to travel. The Stokes-Einstein equation (Siegel and Rathbone, 2012), presented by Equation 2, provides insight into the fundamental properties affecting diffusivity.

$$D = k_B T/6\pi a\mu \qquad (2)$$

Where: $D$ is the diffusivity; kB is Boltzmann's constant; $T$ is the temperature in Kelvin; $a$ is the radius of the molecule; and $\mu$ is the dynamic viscosity of the medium.

It is clear from Equation 2 that there are three properties governing diffusivity:

- The higher the temperature, the higher the diffusivity (more rapid random movements of the molecules).
- The smaller the molecule, the higher the diffusivity.
- The higher the viscosity of the solvent, the lower the diffusivity.

The last point is of concern with polymer systems. If a polymer is considered as a solid, the diffusivity should approach zero according to Equation 2. However, this is not true, because a polymer possesses a so-called micro-viscosity, which is a more accurate parameter to use for diffusivity than the bulk viscosity. This micro-viscosity is explained by the free volume theory, which states that each polymer molecule contains an impenetrable core, surrounded by nano-voids or free volume. The polymer matrix is a dynamic fluctuating structure and so the size of the voids also fluctuates. On occasion, a void size increases to such an extent as to allow a molecule to diffuse through it (Siegel and Rathbone, 2012).

This micro-viscosity in turn is controlled by four variables, namely temperature, the crystallinity of the polymer, the state of the polymer and the sorption of smaller molecules than those of the release substance.

- When the temperature increases, the movement of polymer chains is more intense, therefore an increase in the diffusivity is observed (besides the increased movement of the release substance).
- Crystalline domains in the polymer act as obstructions to the release substance, decreasing available voids and increasing the diffusion path length.
- If the temperature drops below the glass transition temperature of the polymer, the polymer chains become static and there is a drastic decrease in free volume.
- The sorption of small molecules may cause a dry, glassy polymer to convert to a rubbery state (gelling of the polymer), greatly increasing the mobility of the release substance. This is commonly referred to as swelling and the small molecule commonly absorbed is water.

From these variables, it can be concluded that there are two categories according to which controlled release kinetics from a polymeric system can be classified. They are the internal structure (reservoir or monolithic) of the polymeric system and the state of the polymer. The state of the polymer is whether the polymer is gelled (if the polymer is below its glass transition temperature or above it), the dissolution of the polymer and the degradability of the polymer (Siegel and Rathbone, 2012).

### 2.7.2 Internal structures of micro-particles

There are mainly two micro-encapsulation systems possible, namely a reservoir system and a monolithic system, each with a different internal structure. Some authors differentiate between microcapsules and microspheres based on these internal structural differences, where reservoir systems correspond to the former and monolithic systems to the latter. (Anal and Singh, 2007). In this study, micro-particles is regarded as the non-specific term for microcapsules and microspheres.

***Reservoir system***

The characteristics of a reservoir system (microcapsules) are a well-defined core containing the active substance surrounded by a well-defined polymer membrane. Controlled release of the active substance takes place by diffusion of the substance through the polymer membrane; therefore the release kinetics can be explained by Fick's Law. What makes the system of particular interest is that it can display extended zero-order release kinetics under specific conditions, which is the most favoured behaviour (this is discussed in detail in Section 2.8).

There are, however, two disadvantages to the system: reservoir systems tend to be difficult to produce and most likely result in expensive products. In addition, there is the risk of microcapsules rupturing with a consequential sudden release of the active substance resulting in an overdose (Heller and Hoffman, 2004). This should not be confused with the burst release effect discussed in Section 2.8.

***Monolithic system***

In a monolithic system (microspheres) there is no outer membrane, and these systems are in effect matrix devices with the active substance uniformly distributed in the polymer. The release kinetics depend on whether the active substance is dispersed or dissolved, and unlike a reservoir system, zero-order release kinetics is nearly impossible (Siegel and Rathbone, 2012). The advantages of this system, however, are that a sudden release is not possible due to bursting capsules and the production is usually inexpensive (Heller and Hoffman, 2004).

### 2.7.3 State of the polymer

***Gelling***

The gelling of a polymer occurs by means of a process called swelling, i.e the uptake of the medium (usually water) in which the polymer exists; once swelled it is referred to as a hydrogel. The dynamic swelling behavior of hydrogels is controlled by the structure of the polymeric network and polymer–medium interactions. A schematic diagram of the sweliing process is given in Figure 2-5.

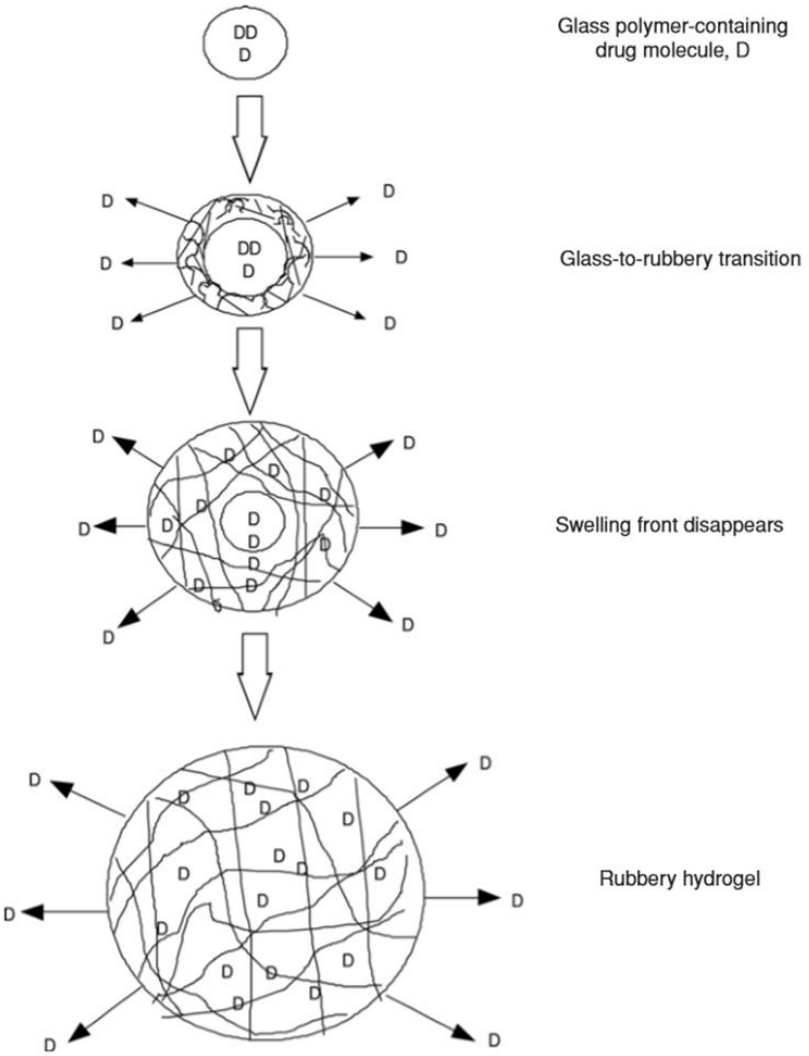


**Figure 2-5: Schematic of the swelling process in a polymer (Onwulata and Huth, 2009).**

Note that in Figure 2-5 there are three distinct states, i.e an unswollen glassy polymer, a polymer in which a swelling front exists, liberating the active substance, and a completely swollen (gelled) polymer. This can mathematically be described by the Deborah number (Ritger and Peppas, 1987) given by Equation 3.

$$D_e = \tau/\vartheta \qquad (3)$$

Where: $\tau$ is the characteristic relaxation time of the polymer and $\vartheta$ is the characteristic diffusion time of the solvent (water) into the polymer. If $D_e << 1$ then the polymer is in a rubbery state, because the polymer immediately relaxes upon solvent uptake. The release kinetics is then Fickian. This is known as Case II transport. If $D_e >> 1$, the polymer is in a glassy state and is diffusion controlled, therefore once again Fickian kinetics are exhibited. If

$D_e \approx 1$, the diffusion and relaxation of the polymer is coupled and the release kinetics are considered non-Fickian.

It should be clear that Fickian behaviour should always be observed with reservoir systems as the active substance is not in a polymer matrix (therefore the active substance is not liberated) and the relaxation of the polymer membrane will only increase the diffusion rate. For monolithic systems, the release behaviour can therefore be Fickian or non-Fickian. A comprehensive summary of the release mechanisms is given in Table 2-5.

**Table 2-5: Comprehensive summary of the mechanisms of controlled release if perfect sink conditions are met.**

| | **Monolithic** | **Reservoir** |
|---|---|---|
| Glassy | Fickian, non-zero order | Fickian, zero order |
| Swelling | Non-Fickian | Mostly Fickian, zero order |
| Swollen | Fickian, approaches zero order | Fickian, zero order |

Note that for the monolithic and the reservoir systems, the release rate will be faster in the case of a swollen matrix or membrane.

## 2.8 Kinetic models of controlled release

***Monolithic systems***

The simplest model for describing the release of an active substance from a monolithic system is the semi-empirical power law model (Siepmann and Peppas, 2001) given by Equation 4.

$$m_r(t)/m_o = (kt)^n \quad (4)$$

Where: $m_r(t)$ and $m_o$ are the absolute cumulative amount of active substance released at time $t$ and infinite time (which should be equal to the total amount captured in the polymer at time $t = 0$); $k$ is a constant incorporating structural and geometric characteristics of the device; and n is the release exponent, indicative of the mechanism of active substance release. The Higuchi model given by Equation 5 is also represented by this model (Higuchi, 1961).

$$\frac{m_r(t)}{A} = \sqrt{D(2c_o - c_s)c_s\, t} \text{ for } c_o > c_s \quad (5)$$

Where: $D$ is the diffusion coefficient; $c_o$ is the initial active substance concentration; $c_s$ is the solubility of the active substance in the polymer; and $A$ is the area exposed to the external medium.

It should be remembered that the assumptions for this model in Equation 5 are that the concentration of the initial active substance is much higher than the solubility of that in the polymer, perfect sink conditions apply, swelling is negligible and the polymer is a thin film. The adjusted values for n are given in Table 2-6 (Siepmann and Peppas, 2001).

**Table 2-6: Adjusted values for n according to mechanism of transport and geometry.**

| Exponent n | | | Release mechanism |
|---|---|---|---|
| Thin film | Cylinder | Sphere | |
| 0.5 | 0.45 | 0.43 | Glassy diffusion |
| 0.5 < n < 1.0 | 0.45 < n < 0.89 | 0.43 < n < 0.85 | Non-Fickian |
| 1.0 | 0.89 | 0.85 | Case-II |

It is clear that a monolithic system can only show zero-order kinetics if it is swollen.

***Reservoir systems***

The kinetics of a reservoir system can be deduced from Fick's first law given by Equation 6.

$$j = -\rho D \frac{dw}{dx} \qquad (6)$$

Where: The mass flux is represented by $j$; the diffusivity by $D$; the mass fraction of a component by $w$; and the membrane thickness by $x$. For a single component system when perfect sink conditions are met and if the membrane thickness equals $x$, and also remains constant with time, then Equation 7 will be true.

$$\frac{dw}{dx} = -1/x \qquad (7)$$

Equation 6, multiplied by the area of the microcapsule on both sides, results in the change in component mass within the microcapsule. Therefore Equation 8 can be deduced.

$$\frac{dm_t}{dt} = -A\rho D/x \qquad (8)$$

Where: $m_t$ is the mass of the volatile remaining in the micro-particles. Upon integration, the zero order kinetic profile can be deduced. This is given by Equation 9.

$$m_t = m_o - (A\rho Dt/x) \qquad (9)$$

Note that ADρ*t*/*x* is the mass released ($m_r$). Also note that this corresponds to Equation 4 where n=1 for zero-order kinetics. Equation 10 shows it in the same format.

$$m_t/m_o = 1 - (ADpt/xm_o)^n \qquad (10)$$

# 3 Experimental

Zein, geraniol and wintergreen oil were purchased from Sigma Aldrich, USA. Ethanol (99%) was purchased from Merck, Germany.

## 3.1 Solubility of zein in an aqueous ethanol mixture

Approximately 300 mg of zein was added to ethanol-water solutions in pre-weighed glass containers with varying ethanol concentrations. The ethanol content varied from 0 to 100% in 10% increments. The ethanol-water solutions were prepared by adding 1 000 mg of anhydrous ethanol (99% pure) to each container, while varying the amount of distilled water added to achieve the required concentrations. After the zein had been added, the mixture was stirred with a commercial kitchen blender for one minute and left for 24 hours for equilibrium to be reached. Two repeats at each ethanol concentration were conducted. The undissolved zein precipitated at the bottom of the containers and was clearly visible due its dark yellow colour; however, some zein particulates remained suspended. The solutions were then filtered using pre-weighed Whatman grade 1 filter paper. The undissolved solids in the containers and those captured with the filter paper were dried in an oven at 50 ˚C for approximately one hour and weighed. Through mass balance calculations the mass of dissolved zein was then approximated.

## 3.2 Preparation of micro-particles

Micro-particles loaded with geraniol and wintergreen oil were prepared using the phase separation method as it was decided to be the simplest and the most practical method for producing large amounts of micro-particles for agricultural use. In both instances, 2 g zein was dissolved in 15.7 ml of an 80% ethanol-water mixture, resulting in a solution containing 15% zein on a mass basis. Either geraniol or wintergreen oil was then added to the solutions in volatile-to-zein mass ratios of 4:1, 3:1, 2:1, 1:1, 1:2 and 1:3. Each solution was stirred for 2 minutes using a kitchen blender to mix the oil in the solution. While stirring, distilled water was instantly added to each solution, resulting in an approximate 70% water mixture and stirred for another minute. The instant addition of water caused the phase separation

of the zein, precipitating out of the solution and encapsulating the oil. All procedures were performed at room temperature.

The geraniol-containing micro-particles floated on the solutions, and the majority were scooped off the surface with a spatula. The remaining particles were filtered out using Whatman grade 6 filter paper, taking care that the precipitated zein which was not involved in the encapsulation, did not dislodge from the bottom. The wintergreen oil-containing micro-particles, however, did not float and were separated from the precipitated zein, which was not involved in the encapsulation, by passing the solution through a 200 µm sieve.

The captured micro-particles were stored at -20 ˚C until further analysis. Four samples of each volatile-to-zein mass ratios were prepared, of which two were used to determine particle yield and the remaining two for all other analyses. For all analyses, except particle yield determination, approximately half of the captured micro-particle mass was lyophilised (i.e. freeze dried). Prior to lyophilisation, the geraniol-containing micro-particles were rinsed with water while being subjected to vacuum filtration using Whatman grade 6 filter paper to remove non-encapsulated oil. The same could not be done for the wintergreen oil as preliminary tests indicated that the wintergreen micro-particles were extremely small and would pass through the filter paper. Consequently, the wintergreen oil micro-particles were centrifuged in an effort to concentrate them. All micro-particles were stored at -60 ˚C for 2 hours and then lyophilised at -60 ˚C to remove all water, ethanol and remaining non-encapsulated oil. The lyophilisation pressure measurements ranged from 100 to 400 mTorr. The geraniol and wintergreen oil micro-particles were lyophilised for 24 hours and 36 hours respectively as water crystals were still clearly visible for the latter case after 24 hours.

## 3.3 Particle yield

For samples used in this instance, special care was taken to recover all the micro-particles. Any capsules adhering to the surface of the container were carefully rinsed off with distilled water prior to filtering. The recovered micro-particles were placed in prior weighed petri dishes and placed in an oven at 50 ˚C for approximately one hour. The micro-particles were dried to the point where they were tangibly dry, but care was taken not to dry out the

micro-particles. With this, the assumption was made that all water, ethanol and non-encapsulated volatiles had been driven off and that a negligible amount of encapsulated volatile was released (this was later confirmed from kinetic studies). The wintergreen oil and the geraniol samples were dried separately to prevent contamination. The petri dishes with their contents were then weighed.

The particle yield is defined as the mass fraction of oil and zein added that participates in the formation of micro-particles. The mathematical description is given by Equation 11.

$$\text{Particle Yield (w/w\%)} = (m_D/m_T) \times 100 \qquad (11)$$

Where: $m_D$ is the mass of the micro-particles after drying; and $m_T$ is the total mass of zein and geraniol or wintergreen oil initially added.

## 3.4 Volatile mass fraction, encapsulation and participation efficiency

Geraniol or wintergreen oil mass fractions, subsequent geraniol or wintergreen oil encapsulation efficiencies and zein participation efficiencies were determined by thermogravimetric analysis (TGA) in a Perkin Elmer 4000 with Pyris software. For the geraniol- and wintergreen-containing micro-particles, samples of 30 and 10 mg respectively were weighed off and placed in 50 µL alumina pans. TGA analysis was performed prior to and after lyophilisation for the geraniol micro-particles, but for the wintergreen micro-particles, analysis was only performed after lyophilisation. The samples were heated at a rate of 10 ˚C/min from 30 to 300˚C. The TGA chamber was continuously purged with nitrogen at 50 ml/min. The inert atmosphere was chosen to prevent the oxidation of the zein and auto-ignition of geraniol that may have affected the observed mass loss.

Volatile mass fraction is defined as the volatile mass fraction of the micro-particles. The mathematical description is given by Equation 12.

$$\text{Volatile mass fraction (w/w\%)} = (m_{EV}/m_{TM}) \times 100 \qquad (12)$$

Where: $m_{EV}$ is the mass of encapsulated volatile; and $m_{TM}$ is the total mass of the micro-particles.

Volatile encapsulation efficiency is defined as the fraction of volatile initially added that participates in the formation of micro-particles. The mathematical description is given by Equation 13.

$$\text{Volatile encapsulation efficiency (w/w\%)} = (m_{PV}/m_{AV}) \times 100 \qquad (13)$$

Where: $m_{PV}$ is the mass of volatile that participated; and $m_{AV}$ is the mass of volatile initially added.

The same definition holds for the zein participation efficiency and is given by Equation 14.

$$\text{Zein participation efficiency (w/w\%)} = (m_{PZ}/m_{AZ}) \times 100 \qquad (14)$$

Where: $m_{PZ}$ is the mass of zein that participated in the formation of micro-particles; and $m_{AZ}$ is the mass of zein initially added.

## 3.5 Particle size analysis

The micro-particle size analysis was performed in a Malvern Mastersizer 3000 instrument prior to lyophilisation. It was attempted to analyse lyophilised micro-particles, but they tended to agglomerate and consequently produced inaccurate results. The geraniol micro-particles used for the particle size analysis were rinsed and filtered through Whatman grade 6 filter paper. This was not done for the wintergreen micro-particles, although the non-participating wintergreen oil was carefully disposed of after centrifuging. Just prior to analysis, the micro-particles were thoroughly dispersed in water by rapidly stirring the mixture to ensure that no agglomeration occurred.

## 3.6 Microscopy

### 3.6.1 Light microscopy

The geraniol- and wintergreen-containing micro-particles were dispersed in small amounts of distilled water and placed on microscopy plates with cover slips. They were viewed with 40x and 100x objectives with a Nikon Optiphot microscope.

### 3.6.2 Scanning electron microscopy

The carbon-coated micro-particles were viewed after lyophilisation, as there were concerns that the non-participating oil could damage the scanning electron microscope (SEM). Afterwards, they were examined with a Zeiss Ultra 55 FESEM field emission scanning electron microscope (FESEM) at an acceleration voltage of 1 kV.

### 3.6.3 Confocal microscopy

Prior to examination, a fluorescein isothiocyanate (FITC) and water mixture (0.1 mg/mL) was added to the micro-particles on a microscopy plate to induce fluorescence of zein. It was left for approximately three minutes to react. The confocal images were taken with a Zeiss 510 META confocal laser scanning microscope, equipped with a 100x oil immersion objective.

## 3.7 Kinetics

The kinetics of the release of geraniol from the micro-particles were determined by TGA analysis in a Perkin Elmer 4000. Samples of 30 mg were accurately weighed off and placed in 50 µL alumina pans. Runs were performed of the geraniol-to-zein mass ratio 3:1 system as it showed the most promising results. A sample was heated from 30 ˚C to 60 ˚C, 70 ˚C and 80 ˚C respectively at a rate of 10 ˚C/min. The sample was then kept at the end temperature until no further mass loss could be detected. The TGA chamber was continuously purged with nitrogen at 50 ml/min to ensure that it approached sink conditions.

Additional runs at 40 ˚C were performed in an oven to improve the mathematical correlation. These runs were not performed in the TGA due to limited booking time available. Silica gel crystals were placed in the oven to ensure that low humidity conditions similar to those in the TGA chamber could be maintained.

# 4 Results and Discussion

## 4.1 Solubility of zein

The experimentally determined solubility of zein in an ethanol-water solvent is shown in Figure 4-1.

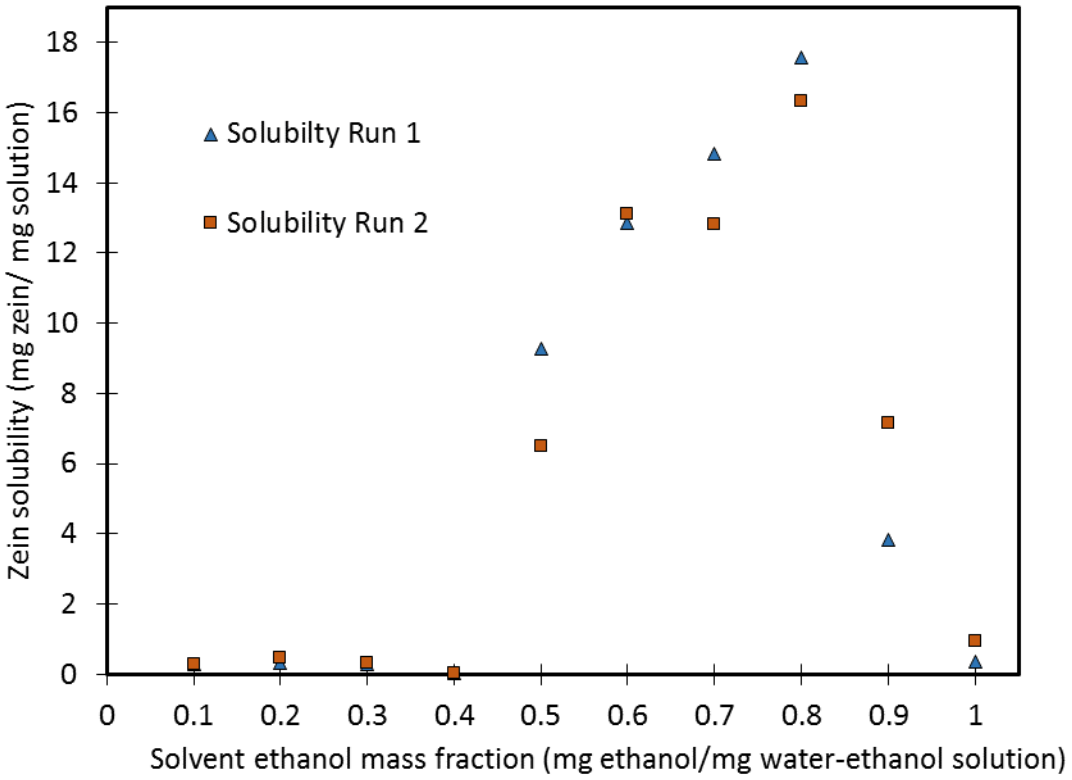


**Figure 4-1: Solubility of zein in an ethanol-water solvent with varying ethanol content.**

From Figure 4-1 the peculiar solubility behaviour of zein can clearly be seen. It is practically insoluble in pure water and pure ethanol. However, a sudden increase in its solubility occurs at a 50% ethanol mass fraction and this solubility range extends up until 80% ethanol where it reaches a maximum. A sudden decrease in solubility at 90% ethanol is then observed. This range corresponds very well to the phase diagram (Mossé, 1961), but the ethanol concentration at which the maximum peak occurs does not correspond and the value of the maximum solubility is much less. The phase diagram suggests that the

solubility can be as high as 60%, whereas the maximum in this study never exceeded 18% (Mossé, 1961). The solubility and final mass fractions of the zein solutions in Figure 4-1 are summarised in Table 4-1.

**Table 4-1: Mass fractions of the components in the zein-ethanol-water solution.**

| **Ethanol mass fraction in solvent (mg ethanol/mg solvent)** | **Zein mass fraction in solution (mg zein/ mg solution)** | | | |
|---|---|---|---|---|
| | Run 1 | Run 2 | Average | Standard deviation |
| 1 | 0.004 | 0.009 | 0.007 | 0.003 |
| 0.9 | 0.038 | 0.071 | 0.055 | 0.017 |
| 0.8 | 0.176 | 0.163 | 0.169 | 0.006 |
| 0.7 | 0.148 | 0.128 | 0.138 | 0.10 |
| 0.6 | 0.129 | 0.131 | 0.13 | 0.001 |
| 0.5 | 0.093 | 0.065 | 0.079 | 0.013 |
| 0.4 | 0.000 | 0.000 | 0.000 | 0.000 |
| 0.3 | 0.003 | 0.003 | 0.003 | 0.000 |
| 0.2 | 0.003 | 0.005 | 0.004 | 0.001 |
| 0.1 | 0.003 | 0.003 | 0.003 | 0.000 |

The zein-ethanol-water solution in all the micro-particle preparations are based on the findings summarised in Table 4-1. Therefore an ethanol solvent mass fraction of 80% was used and the ultimate zein-ethanol-water solutions contained 15% zein. The zein mass fraction was slightly decreased as a contingency measure.

## 4.2 Particle yield

### 4.2.1 Zein-geraniol system

The formation of micro-particles in this system could be visually observed. A light yellow viscous cream formed on top of the solvent medium of the batches that yielded significant amounts of micro-particles. Initial light microscopy confirmed that the cream consisted of micro-particles. This is shown in Figure 4-2.

The fact that the cream floated on top of the solvent was the first indication that the geraniol was successfully encapsulated and the micro-particles did not merely consist of zein or water encapsulated in the zein. This is due to the low density of the geraniol with an SG of 0.879, whereas zein that did not participate collected at the bottom (SG 1.25). The precipitated zein could easily be distinguished by the darker yellow colour. The particle yields obtained for the different geraniol-to-zein mass ratios are given in Table 4-2.

**Table 4-2: Particle yields of different geraniol-to zein mass ratio systems.**

| Geraniol-to-zein mass ratio | Particle yield (mg/mg%) | | | | |
|---|---|---|---|---|---|
| | Run 1 | Run 2 | Run 3 | Average | Standard deviation |
| 4:1 | 80.9 | 84.0 | 75.6 | 80.2 | 2.9 |
| 3:1 | 83.4 | 84.9 | 87.6 | 85.3 | 1.8 |
| 2:1 | 81.7 | 73.7 | 83.2 | 79.5 | 4.2 |
| 1:1 | 0.4 | 0.2 | 0.0 | 0.2 | 0.1 |
| 0.5:1 | 0.3 | 0.5 | 0.3 | 0.4 | 0.1 |
| 0.33:1 | 0.4 | 0.2 | 0.2 | 0.3 | 0.1 |

The geraniol-to-zein mass ratio of 3:1 showed the highest particle yield throughout all the repetitions with an average of 85.3%. A very interesting phenomenon occurs at a geraniol-to-zein mass ratio of 1:1, where ratios equal to or lower than this showed almost no particle yield, with the highest average being a mere 0.4% for the 0.5:1 mass ratio. In contrast, mass ratios higher than this showed an abrupt increase in particle yield – all were higher than 70%. Therefore there is a clear discontinuity in the particle yield. The abrupt increase in particle yield could also be observed visually. This is shown in Figure 4-2.

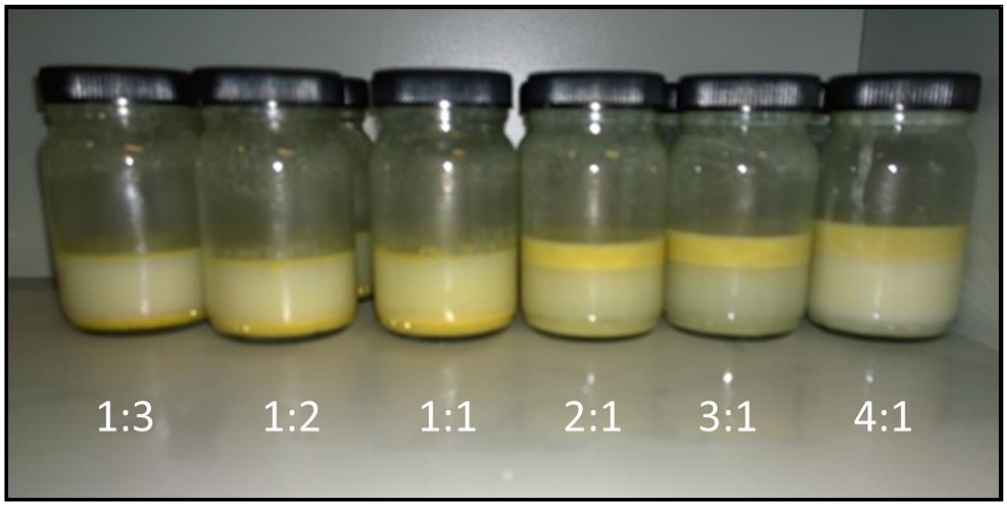


**Figure 4-2: Visual change in particle yield at different geraniol-to-zein mass ratios.**

To obtain a greater understanding of the mechanism of this phenomenon, geraniol solubility tests were conducted. These showed that the mass geraniol used in all mass geraniol-to-zein mass ratios, was completely miscible in the 80% ethanol-water solutions prepared. Solutions prepared with zein and without the addition of water also remained stable. However, the mass geraniol used in all geraniol-to-zein mass ratios, was immiscible in ethanol-water solutions with 25% and lower ethanol content. This corresponded to the end ethanol content after the addition of water. Therefore the mixing before the addition of water, did not result in an emulsion, but a solution. Upon the addition of water, the geraniol and the zein then separated from the ethanol-water solutions. At geraniol-to-zein mass ratios of 1:1 and lower, the zein and the geraniol separated separately, but at higher ratios the zein was able to encapsulate the geraniol. Two theories are proposed in this work to explain this phenomenon.

The first theory is that the explanation for the solubility behaviour of zein in an ethanol-water solvent medium may be analogous to the explanation of this abrupt increase of the particle yield depending on the amount of geraniol in the system. If each zein molecule acts as an amphiphile and zein forms macromolecular micelle structures, the hydrophilic moieties will be exposed to the surface with the hydrophobic moieties clumped together (Wang et al., 2004a). If the solvent medium turns hydrophobic, then the orientation of each molecule will be reversed. Therefore a micellar inversion takes place depending on the condition of the solvent medium. The hydrophilic moieties are orientated outwards at

ethanol concentrations lower than 90%, and an inversion takes place at ethanol concentrations higher than 90%, causing the zein to precipitate (Kim and Xu, 2008).

As can be seen from Table 2-3, the dipole moment of geraniol is 1.348 D, showing that it is much less polar than that of water at 1.8546 D and ethanol at 1.69 D (Dipole Moment). Consequently, the addition of geraniol to the solvent medium will cause the environment in which the zein micelles exist to become more hydrophobic. It may be concluded that at geraniol-to-zein mass ratios lower than 2:1, the hydrophilic moieties may still be oriented outwards at an ethanol concentration of 80%, and the presence of geraniol at this stage did not affect this. Since geraniol is hydrophobic (non-polar), the interaction between the geraniol and the hydrophilic zein moieties would be insignificant during phase separation with the addition of water. Therefore the zein precipitates out separately, not encapsulating the geraniol, and a very low particle yield is observed at these mass ratios.

To the contrary, at geraniol-to-zein mass ratios equal to or higher than 2:1, there may be enough geraniol in the solvent medium to cause a micelle inversion, resulting in the hydrophobic moieties to be oriented outwards. There could then be significant interaction between the geraniol and the zein for the geraniol to be encapsulated upon the addition of water.

Furthermore, the high particle yield in a non-polar environment suggests that the zein is mostly non-polar, as expected due to its composition and the fact that the expected major fraction of the zein is α-zein.

The second theory is that due to the increased geraniol activity and decreased zein activity as the geraniol-to-zein mass ratios are increased, the separation kinetics of the two substances may be affected upon the addition of water. At lower geraniol-to-zein mass ratios the zein may precipitate first, followed by the phase separation of geraniol, resulting in poor encapsulation. At higher geraniol-to-zein mass ratios the geraniol may phase separate first and due to the continued stirring, be emulsified. This is then followed by the precipitation of the zein enabling encapsulation.

### 4.2.2 Zein-wintergreen system

For this system, on the addition of water, two distinctive zein-containing phases were observed. Firstly, at all wintergreen-to-zein mass ratios investigated, a large amount of zein precipitated out as a sticky, dark yellow mass collecting at the bottom of the container. It was therefore visually evident that low particle yields could be expected. The second phase consisted of a white to yellow colour solid that appeared to have fluid-like properties if shaken, suggesting that it consisted of small particles (this was confirmed with microscopy). These micro-particles, unlike the geraniol micro-particles, collected at the bottom of the container. Therefore it could not be concluded whether the wintergreen was encapsulated or not since the SG of wintergreen is 1.18. The precipitated zein and micro-particles are shown in Figure 4-3 and the particle yields obtained are given in Table 4-3.

**Figure 4-3: Precipitated zein and micro-particles formed after phase separation in the wintergreen oil-zein system.**

**Table 4-3: Particle yields of different wintergreen-to-zein mass ratio systems.**

| Wintergreen-to-zein mass ratio | Particle yield (mg/mg %) | | | | |
|---|---|---|---|---|---|
| | Run 1 | Run 2 | Run 3 | Average | Standard deviation |
| 4:1 | 22.50 | 20.94 | 7.90 | 17.11 | 6.55 |
| 3:1 | 8.47 | 12.59 | 5.38 | 8.81 | 2.95 |
| 2:1 | 6.35 | 8.59 | 5.50 | 6.81 | 1.30 |
| 1:1 | 11.67 | 10.07 | 8.75 | 10.16 | 1.19 |
| 0.5:1 | 13.50 | 12.50 | 17.33 | 14.45 | 2.08 |
| 0.33:1 | 10.5 | 19.01 | 16.88 | 15.46 | 3.62 |

As can be seen from Table 4-3, the particle yields are indeed much lower than the geraniol-zein system. The highest particle yield achieved was 22.5% for a wintergreen-to-zein mass ratio of 4:1. Furthermore, the results seem to be inconsistent with no definite trend. By disregarding mass ratios 3:1 (although in run 2 it did show a similar value) and 2:1, the particle yield seems not to vary that much.

Similar wintergreen solubility tests were conducted and similar results were obtained i.e. the mass wintergreen oil used in all wintergreen-to zein mass ratios were completely miscible in the 80% ethanol-water solutions prepared, but immiscible in 25% and lower ethanol-water solutions. However, solutions containing zein, without the addition of water did not remain stable where zein and wintergreen oil separated. Precipitated zein and wintergreen oil droplets were collected at the bottom of the containers.

By taking into account that the dipole moment of methyl salicylate (the major constituent of wintergreen) is 2.47 D compared to that of water at 1.8546 and ethanol at 1.69 D

(Lide, 2004), it can be considered to be relatively polar. Since zein is mostly non-polar, it seems that the interaction between the zein and the wintergreen oil is not favourable to result in encapsulation. However, the fact that micro-particles did form, may suggest that a certain fraction of zein other than α-zein participated.

## 4.3 Volatile mass fraction

### 4.3.1 Zein-geraniol system

TGA runs of the micro-particles were performed prior to and after lyophilisation to estimate the differences in geraniol mass fractions due to lyophilisation. Assuming that no zein is lost, the fraction of oil lost during lyophilisation can be estimated. Three approaches were followed to estimate the geraniol content of the micro-particles prior to lyophilisation. The first case approach was to assume that any mass loss observed below the boil-off temperature of pure water at the relevant pressure was only due to water or ethanol. Therefore no geraniol was lost at these low temperatures. The second case approach was to assume that if geraniol was lost at these low temperatures, the fraction of geraniol lost up to the boil-off temperature of pure water, should equal the fraction of geraniol lost in the case of only pure geraniol. These assumptions were made due to the significant difference in the volatility of water or ethanol compared to the volatility of geraniol and its immiscibility with water. The third approach was based on thermodynamic calculations, where the composition of the mass loss was approximated by the application of Raoult's Law. Please refer to Appendix I for a detailed discussion on the thermodynamic approach. It should be noted that the assumptions for the thermodynamic approach were that the system reaches steady state and is closed, which is not accurate. Therefore the three approaches are followed to indicate the possible variance in the true geraniol mass fractions.

#### 4.3.1.1 Geraniol-to-zein mass ratio 2:1

***Experimental approach prior to lyophilisation***

The TGA results of the micro-particles prior to lyophilisation are shown in Figure 4-4. The mass loss curves of the pure substances involved in the preparation are also included.

The first matter of concern is that a heterogenic azeotrope may be reached, since the geraniol is immiscible with the ethanol-water phase at the end preparation compositions. Depending on the composition of the micro-particles, the liquid phase may either approach pure geraniol or pure solvent (water and ethanol) as they are heated. Consequently, the boiling point temperature of the liquid phase will also approach the boiling point

temperature of either of the two at the relevant pressure. From Figure 4-4 it is clear that a significant mass loss occurs beyond the boil-off temperature of the pure water and the ethanol, indicating that the liquid phase approached pure geraniol. This was proven by thermodynamic calculations (Appendix I).

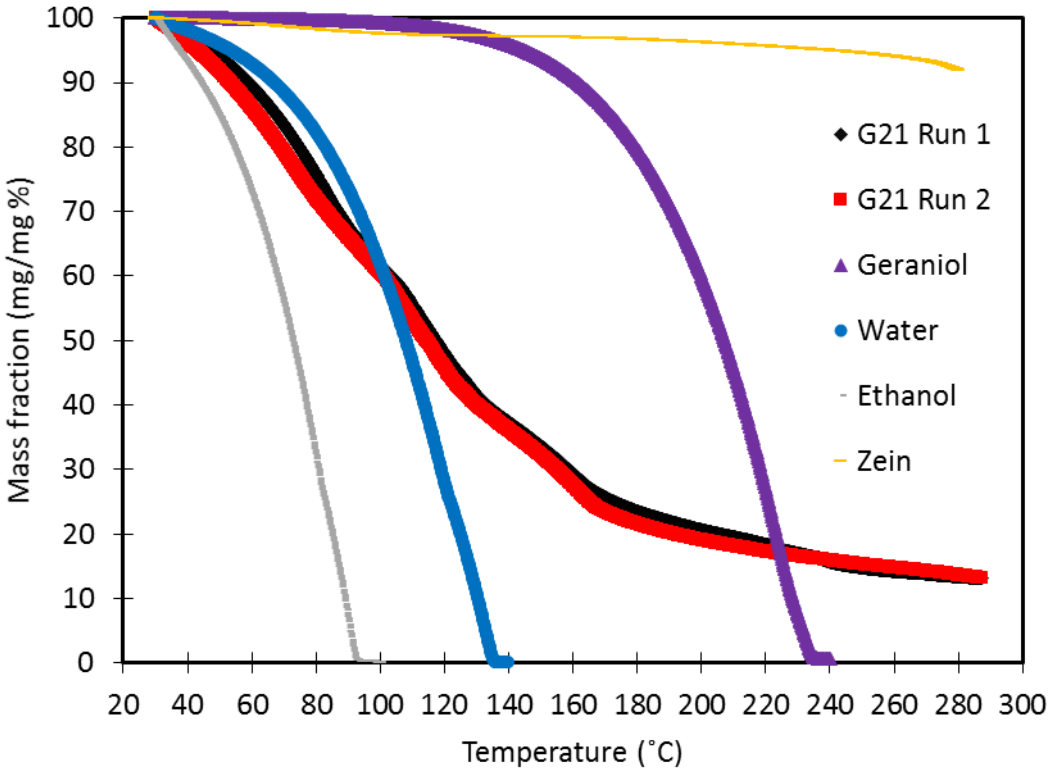


**Figure 4-4: TGA mass loss of geraniol-to-zein mass ratio 2:1 micro-particles at different temperatures prior to lyophilisation.**

By considering the pure substances in Figure 4-4, it can be seen that the onset of mass reduction of the pure zein sample occurs at the highest temperature of approximately 270 ˚C and is higher than the range at which the mass reduction of the zein-geraniol micro-particles stabilised. Therefore it can be concluded that the thermal degradation of zein was not reflected in the mass reduction of the geraniol-zein micro-particles at temperatures lower than 270 ˚C. It is noteworthy that the measured thermal degradation point, at 270 ˚C is much lower than the reported 320 ˚C. Furthermore, the mass reduction onset temperature and the boil-off temperature of the pure geraniol are approximately 107 ˚C

and 233 ˚C respectively. All pure water should be boiled off at a temperature of 135 ˚C and likewise pure ethanol at 90 ˚C.

It can be concluded that the mass reduction of the micro-particles from temperatures of 30 ˚C - 90 ˚C can be attributed to ethanol and water, from 90 ˚C - 107 ˚C to water only, from 107 ˚C - 135 ˚C water and geraniol, and 135 ˚C - 270 ˚C geraniol only. However, it should be noted that since these are the mass loss curves of pure substances, neither the influence of the interaction between the substances on the mass loss nor the diffusion of the substances through the polymer is taken into account.

The mass loss rate in Figure 4-5 clearly shows the ranges at which different substances are evaporated with three distinct peaks. The first peak indicates the mass loss of ethanol and water with a maximum mass loss rate at approximately 72 ˚C, corresponding to the boiling point of ethanol. Thereafter a decrease in the mass loss rate is observed, and it is noted that all the ethanol has been boiled off, followed by an abrupt increase in the mass loss rate at a temperature of 97 ˚C, which corresponds to the boiling point of water. The third peak resembles the mass loss of the geraniol.

From this, an approximation of the geraniol mass fraction can be established. The geraniol mass loss taken only from 135 ˚C for run 2 is 26.2 % of the total observed mass loss. A geraniol mass fraction of 62.6% then follows. However, from Figure 4-4, the geraniol mass loss up until 135 ˚C is approximately 3.6% of the geraniol contained. By taking this into account the geraniol mass fraction increases to 63.3%. The results for Run 1 and Run 2 are summarised in Table 4-4 at the end of this section.

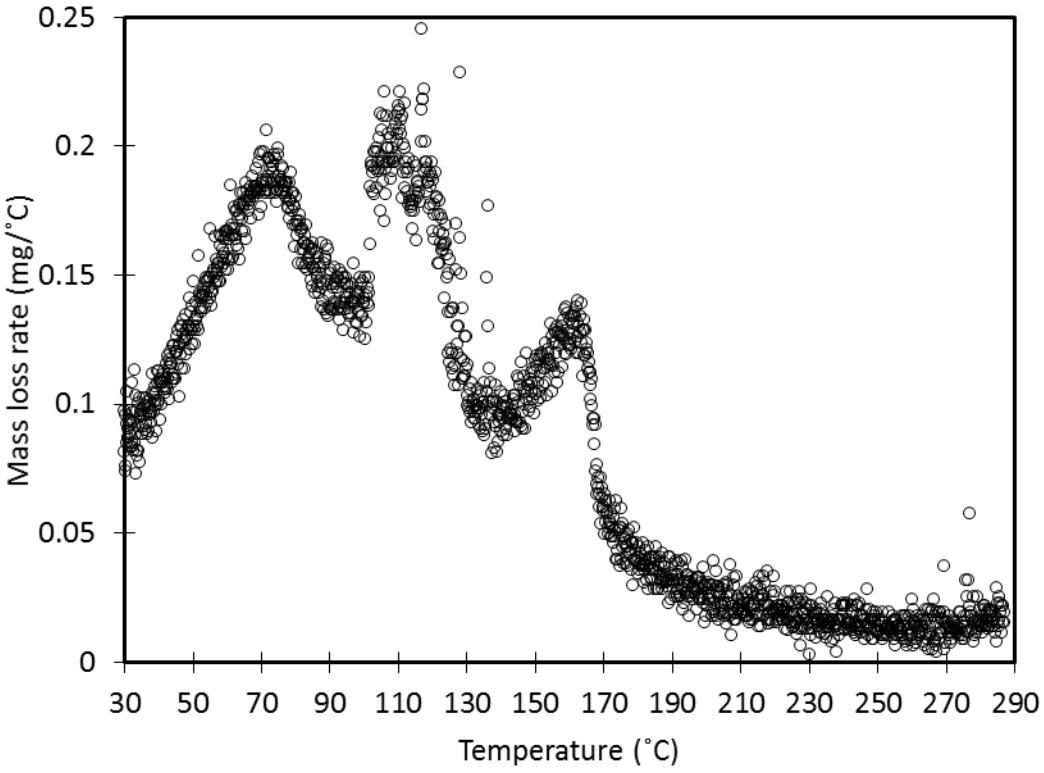


**Figure 4-5: TGA mass loss rate of geraniol-to-zein mass ratio 2:1 micro-particles at different temperatures prior to lyophilisation.**

***Thermodynamic approach prior to lyophilisation***

The predicted remaining mass of the subsequent substances are shown in Figure 4-6. The respective temperatures predicted at which ethanol and water are completely boiled off are 95 ˚C and 105 ˚C.

For comparison, the mass loss rates of the different substances are shown in Figure 4-7. As expected, the first peak can be attributed to the increasing mass loss rates of ethanol and water, after which the water loss rate flattens out with an abrupt increase close to its boiling point, giving rise to the second peak. At this point an increasing contribution from the geraniol mass loss rate is observed. At temperatures exceeding 105 ˚C the mass loss rate can only be attributed to the loss of geraniol, resulting in the third peak of Figure 4-5.

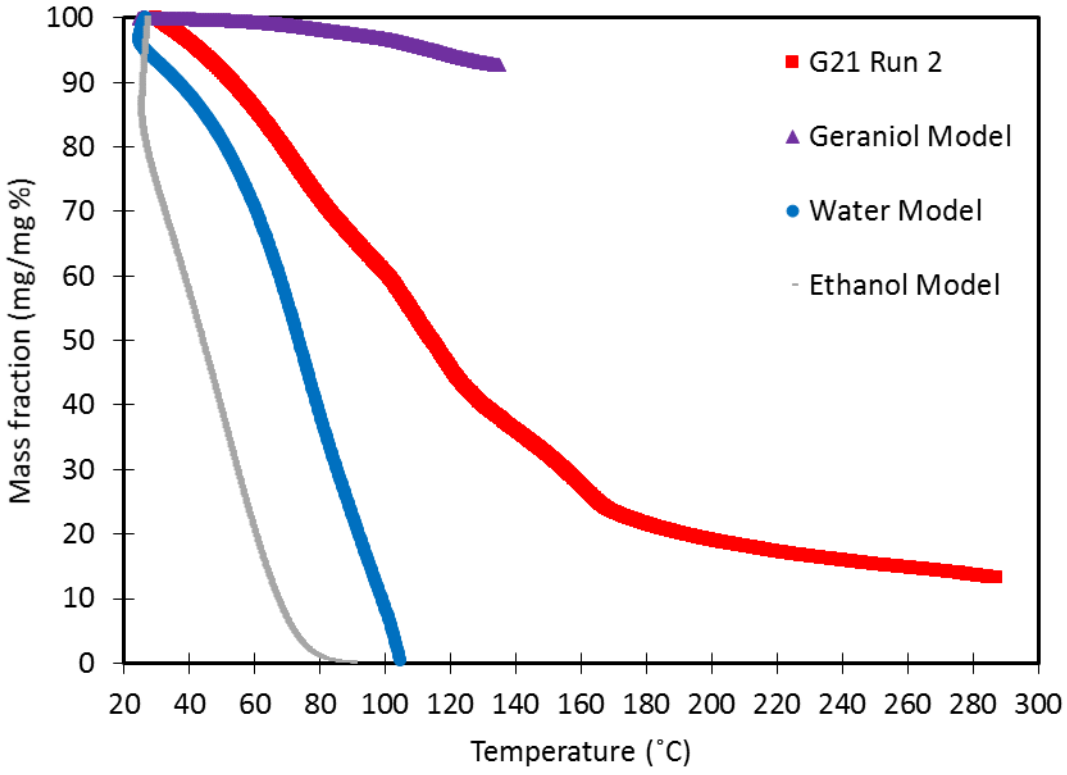


**Figure 4-6: Predicted ethanol, water and geraniol mass remaining at different temperatures prior to lyophilisation for the geraniol-to-zein mass ratio 2:1 system.**

From Figure 4-6, the geraniol mass loss up to 135 ˚C is 7.3% of the total geraniol contained, resulting in a geraniol mass fraction of 66.3%. The best and worst cases are summarised in Table 4-4 at the end of this section.

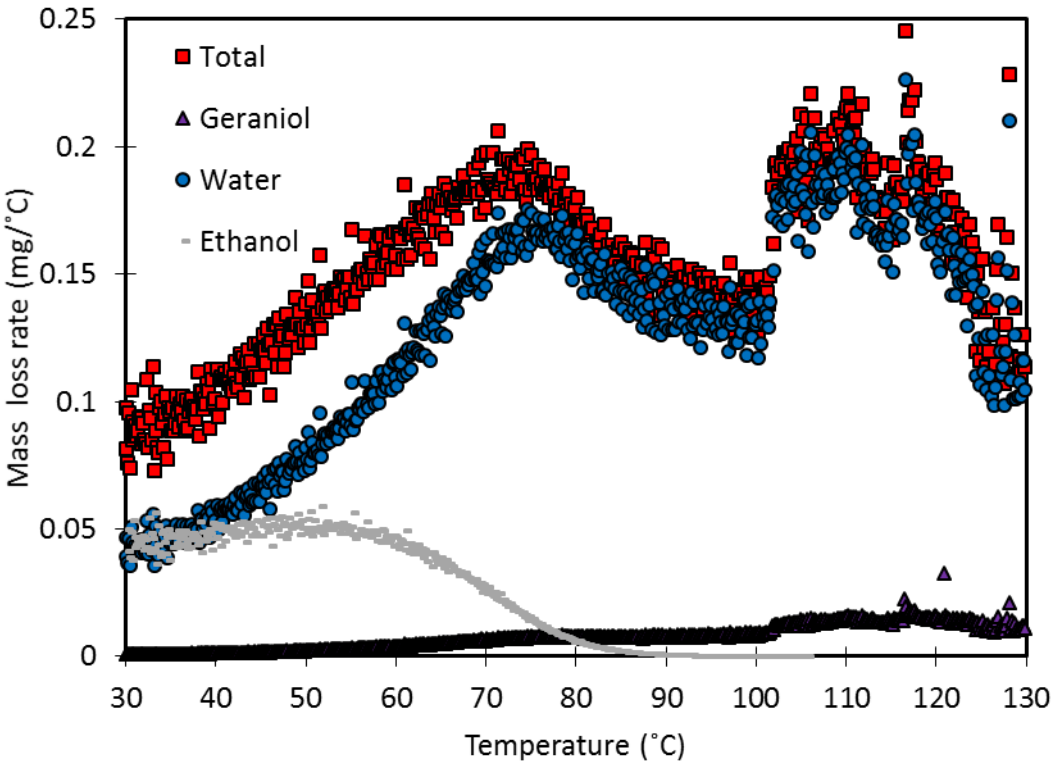


**Figure 4-7: Predicted ethanol, water and geraniol mass loss rates at different temperatures prior to lyophilisation for the geraniol-to-zein mass ratio 2:1 system.**

***Experimental approach after lyophilisation***

The TGA results of the micro-particles after lyophilisation are shown in Figure 4-8.

It is clear from Figure 4-8 that the entire mass loss of the micro-particles at temperatures lower than 270 ˚C can only be attributed to the loss of geraniol. If some water is possibly still present, its contribution to the mass loss should be negligible. The gradient of the mass loss also seems to have abrupt changes. This is confirmed by the rate of mass loss presented in Figure 4-9, which shows three peaks. This should not be confused with the three peaks identified for the micro-particle mass loss prior to lyophilisation.

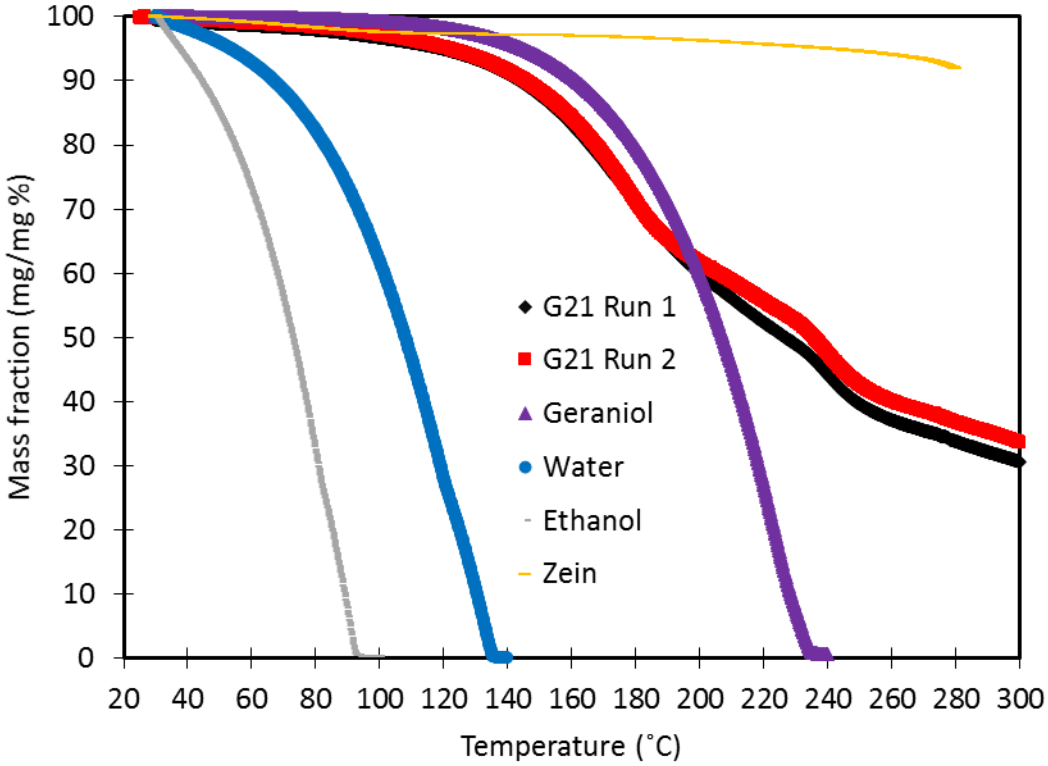


**Figure 4-8: TGA mass loss of geraniol-to-zein mass ratio 2:1 micro-particles at different temperatures after lyophilisation compared to pure component mass loss.**

The third peak in Figure 4-9 is simply the decomposition of the zein polymer with an onset temperature of approximately 272 ˚C, corresponding to the onset decomposition temperature of the pure zein sample from Figure 4-4.

With regard to the geraniol mass loss rate, the first observation is that the temperature at which the geraniol micro-particle is boiled off is much higher than the temperature at which the pure geraniol is boiled of at 265 ˚C compared to 233 ˚C. This is an indication that the geraniol is not merely surface oil, but is encapsulated (the mass loss is not only dependent on the vapour pressure of the geraniol but on the diffusion of the geraniol through the polymer structure). Furthermore, a second geraniol mass loss peak is observed commencing at 220 ˚C. A possible explanation for this is that the geraniol has reached its boiling point (literature value of 230 ˚C), possibly leading to the rupturing of the micro-particles. Consequently there is a rapid release of the remaining oil.

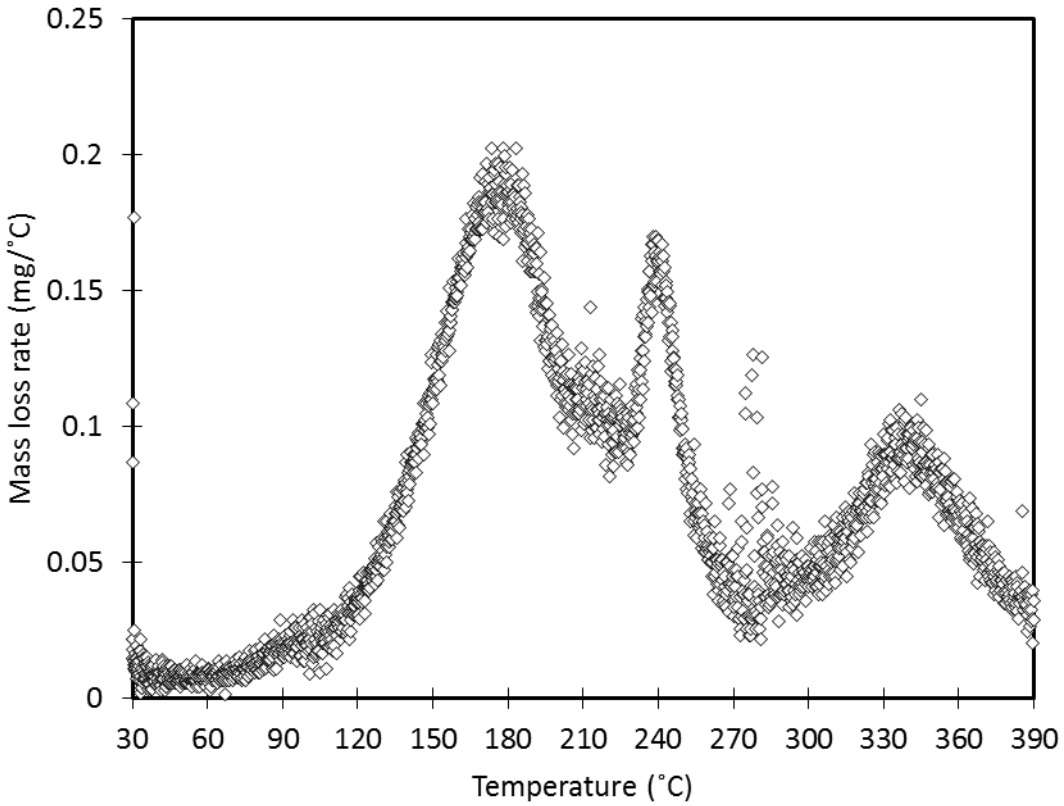


**Figure 4-9: TGA mass loss rate of geraniol-to-zein mass ratio 2:1 micro-particles at different temperatures after lyophilisation.**

The geraniol mass fractions for the geraniol-to-zein ratio 2:1 micro-particles is summarized in Table 4-4.

**Table 4-4: Geraniol mass fractions predicted for the geraniol-to-zein mass ratio 2:1 system with experimental and thermodynamic approaches prior to and after lyophilisation.**

| | Geraniol mass fraction | | | |
|---|---|---|---|---|
| | I | II | III | IV |
| Run 1 | 64.6 | 65.3 | 66.3 | 61.5 |
| Run 2 | 62.6 | 63.3 | 64.3 | 64.5 |
| Average | 63.5 | 64.3 | 65.3 | 63.0 |
| Standard deviation | 0.9 | 1.0 | 1.0 | 1.5 |

I = without lost geraniol, II = with experimental lost geraniol, III = with thermodynamically predicted lost geraniol, IV = after lyophilisation.

From Table 4-4 the geraniol lost during lyophilisation can be estimated. A best, medium and worst case scenario can be defined, corresponding to columns I, II and III of Table 4-4 respectively. The best-case scenario is that only 0.8% of the geraniol originally encapsulated is lost during lyophilisation. The medium and worst case scenarios amount to 2.0% and 3.5% of the geraniol being lost respectively.

By taking into account the particle yields in Section 4.2 and the geraniol mass fractions, the average geraniol encapsulation efficiency and the zein participation efficiency can be estimated. Once again, the efficiencies depend on the amount of geraniol lost during lyophilisation and the accuracy of the calculated mass fractions. The results are presented in Table 4-5.

**Table 4-5: Average geraniol encapsulation and zein participation efficiencies for the geraniol-to-zein mass ratio 2:1 system.**

| Geraniol encapsulation and zein participation efficiency | | | | |
|---|---|---|---|---|
| | I | II | III | IV |
| Zein participation efficiency (%) | 87.1 | 85.1 | 82.8 | 88.2 |
| Geraniol encapsulation efficiency (%) | 75.7 | 76.7 | 77.9 | 75.1 |

I = without lost geraniol, II = with experimental lost geraniol, III = with thermodynamically predicted lost geraniol, IV = after lyophilisation.

#### 4.3.1.2 Geraniol-to-zein mass ratio 3:1

The TGA results for the geraniol-to-zein mass ratio 3:1 micro-particles prior to lyophilisation are shown in Figure 4-10. The thermodynamically predicted mass loss of the different components are also shown.

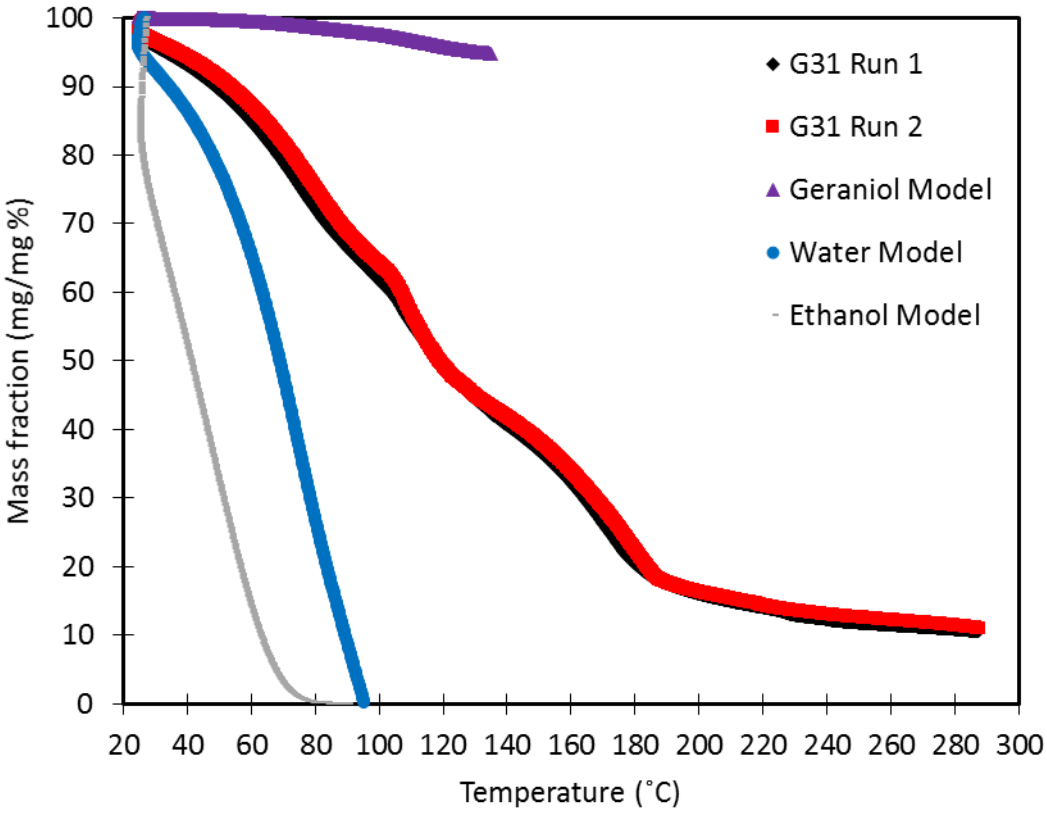


**Figure 4-10: TGA mass loss of geraniol-to-zein mass ratio 3:1 micro-particles at different temperatures prior to lyophilisation with predicted remaining ethanol, water and geraniol mass.**

From Figure 4-10, by referring to the gradient of the mass loss curve of Runs 1 and 2, it is once again clear that there are three distinct regions of mass loss. The same second case approach is taken as for the geraniol-to-zein mass ratio 2:1 micro-particles, i.e. 3.6% of the geraniol is lost at a temperature of 135 ˚C. The geraniol fraction predicted to be lost at 135 ˚C for the geraniol-to-zein mass ratio of 3:1 is 5.1% compared to the 7.3% of the 2:1 system. The geraniol mass fractions prior to lyophilisation are summarised in Table 4-6.

The TGA results for the geraniol-to-zein mass ratio 3:1 micro-particles after lyophilisation are shown in Figure 4-11.

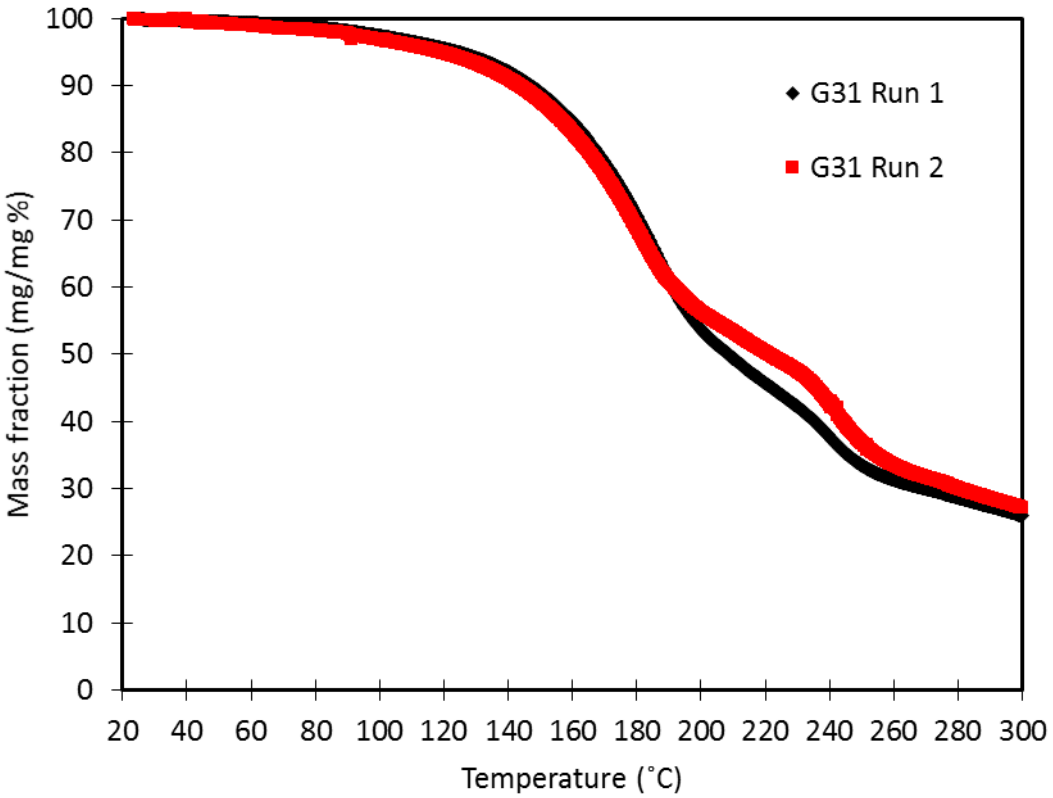


**Figure 4-11: TGA mass loss of geraniol-to-zein mass ratio 3:1 micro-particles at different temperatures after lyophilisation.**

As with the geraniol-to-zein 2:1 system, it is clear that the mass loss observed at a temperature lower than 270 ˚C can only be attributed to geraniol. These micro-particles also show a change in the mass loss rate (three peaks), with the second peak commencing at 210 ˚C. The geraniol mass fractions calculated after lyophilisation are also given in Table 4-6.

**Table 4-6: Geraniol mass fractions predicted for the geraniol-to-zein mass ratio 3:1 system with experimental and thermodynamic approaches prior to and after lyophilisation.**

| | Geraniol mass fraction | | | |
|---|---|---|---|---|
| | I | II | III | IV |
| Run 1 | 76.0 | 76.6 | 76.9 | 70.1 |
| Run 2 | 72.7 | 73.3 | 73.8 | 68.3 |
| Average | 74.4 | 75.0 | 75.4 | 69.2 |
| Standard deviation | 1.65 | 1.65 | 1.55 | 0.9 |

I = without lost geraniol, II = with experimental lost geraniol, III = with thermodynamically predicted lost geraniol, IV = after lyophilisation.

From Table 4-6, the average estimates of the geraniol lost during lyophilisation for the best, medium and worst case scenarios are 7.0%, 7.7% and 8.2% respectively. In all three cases the geraniol lost for the geraniol-to-zein mass ratio 3:1 system is higher than that of the geraniol-to-zein 2:1 system. The geraniol encapsulation and zein participation efficiencies are given in Table 4-7.

**Table 4-7: Average geraniol encapsulation and zein participation efficiencies for the geraniol-to-zein mass ratio 3:1 system.**

| | Geraniol encapsulation and zein participation efficiency | | | |
|---|---|---|---|---|
| | I | II | III | IV |
| Zein participation efficiency (%) | 87.5 | 74.1 | 72.9 | 91.6 |
| Geraniol encapsulation efficiency (%) | 84.5 | 90.4 | 90.9 | 83.5 |

I = without lost geraniol, II = with experimental lost geraniol, III = with thermodynamically predicted lost geraniol, IV = after lyophilisation.

By comparing the geraniol-to- zein mass ratio system 2:1, it seems as if a trend can be observed. Firstly, there is great increase in the geraniol mass fraction, and secondly there is an increase in the geraniol encapsulation and zein participation efficiencies.

#### 4.3.1.3 Geraniol-to-zein mass ratio 4:1

The TGA results for the geraniol-to-zein mass ratio 4:1 micro-particles prior to lyophilisation are shown in Figure 4-12. The thermodynamically predicted mass loss of the different components are also shown.

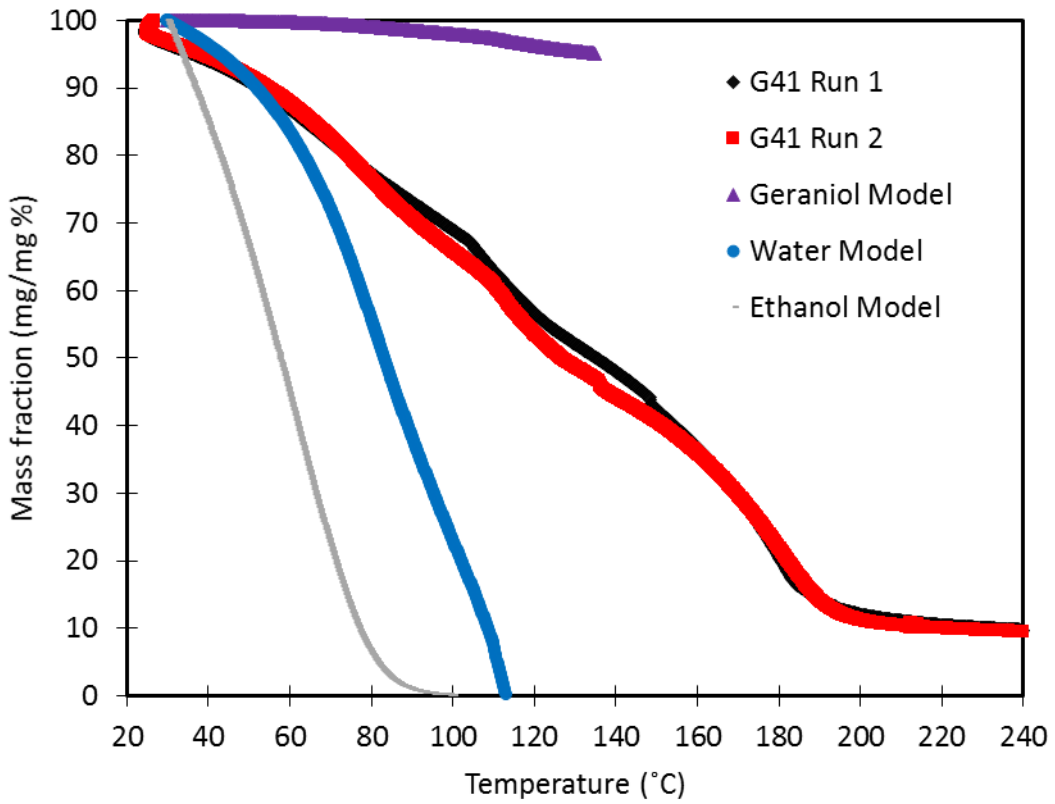


**Figure 4-12: TGA mass loss of geraniol-to-zein mass ratio 4:1 micro-particles at different temperatures prior to lyophilisation with predicted remaining ethanol, water and geraniol mass.**

From Figure 4-12, the gradients of Runs 1 and 2 once again clearly resemble the three peaks observed. From this, the thermodynamically predicted percentage geraniol lost at temperatures lower than 135 ˚C amounts to 4.9%.

The TGA results for the geraniol-to-zein mass ratio 4:1 micro-particles after lyophilisation are shown in Figure 4-13.

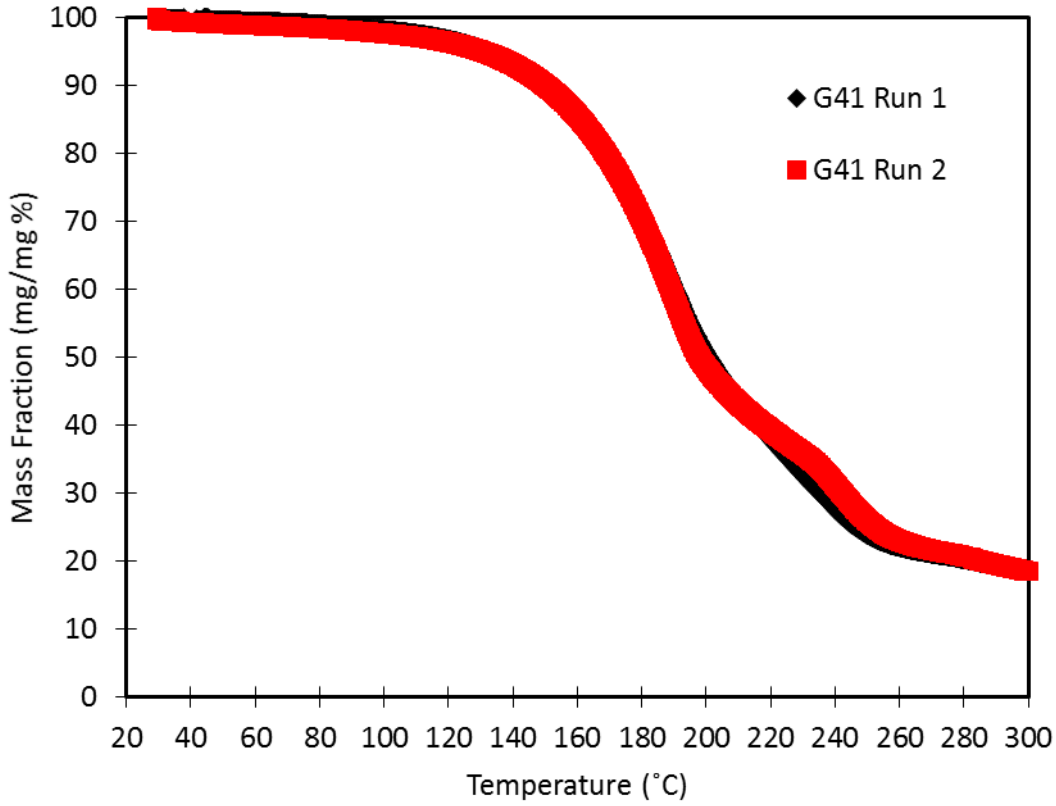


**Figure 4-13: TGA mass loss of geraniol-to-zein mass ratio 4:1 micro-particles at different temperatures after lyophilisation.**

From Figure 4-13, as with the other systems, it is clear that all the water and ethanol was removed during lyophilisation. Another consistency is that the three peaks in the mass loss rate are once again observed, showing a sudden release of the remaining geraniol at a temperature of 212 ˚C. A summary of the geraniol mass fractions for the geraniol-to-zein mass ratio 4:1 is given in Table 4-8.

From Table 4-8, the estimated geraniol lost during lyophilisation amounts to 3.8%, 4.3% and 4.6% for the best, medium and worst case scenarios respectively. The corresponding calculated geraniol encapsulation and zein participation efficiencies are given in Table 4-9.

**Table 4-8: Geraniol mass fractions predicted for the geraniol-to-zein mass ratio 4:1 system with experimental and thermodynamic approaches prior to and after lyophilisation.**

| | Geraniol mass fraction | | | |
|---|---|---|---|---|
| | I | II | III | IV |
| Run 1 | 82.3 | 82.7 | 83.0 | 79.0 |
| Run 2 | 81.2 | 81.6 | 82.0 | 78.4 |
| Average | 81.8 | 82.2 | 82.5 | 78.7 |
| Standard deviation | 0.6 | 0.6 | 0.5 | 0.3 |

I = without lost geraniol, II = with experimental lost geraniol, III = with thermodynamically predicted lost geraniol, IV = after lyophilisation.

**Table 4-9: Average geraniol encapsulation and zein participation efficiencies for the geraniol-to-zein mass ratio 4:1 system.**

| | Geraniol encapsulation and zein participation efficiency | | | |
|---|---|---|---|---|
| | I | II | III | IV |
| Zein participation efficiency (%) | 73.2 | 71.6 | 70.1 | 85.4 |
| Geraniol encapsulation efficiency (%) | 81.9 | 82.3 | 82.7 | 78.9 |

I = without lost geraniol, II = with experimental lost geraniol, III = with thermodynamically predicted lost geraniol, IV = after lyophilisation.

By comparing the 2:1, 3:1 and 4:1 systems, a clear trend is observed, i.e. the mass fraction geraniol significantly increases with the amount of geraniol initially added relative to the amount of zein initially added. Post-lyophilisation geraniol mass fractions increased on average by 9.8% from the 3:1 system compared to the 2:1 system and 24.9% with the 4:1 system compared to the 2:1 system. Therefore the more hydrophobic the environment, the more geraniol is encapsulated.

However, by considering the zein participation efficiency, peculiar behaviour is observed. Initially the zein participation efficiency increases from the 2:1 to the 3:1 system, but

decreases again for the 4:1 system. The same is observed for the geraniol encapsulation efficiencies. In a trade-off of the systems:

- The 4:1 system is the most effective in terms of geraniol mass fraction, second most effective in terms of geraniol encapsulation efficiency but the least effective in terms of zein participation efficiency.
- The 3:1 system is most effective in terms of geraniol encapsulation and zein participation efficiencies and second most efficient in terms of geraniol mass fraction.

In conclusion, by considering the input materials wasted, the 3:1 system will be the most economically feasible, except where the added value of the higher fraction geraniol in the 4:1 system exceeds the value of the wasted input materials. For this reason, only the kinetics of the 3:1 system were studied.

### 4.3.2 Zein-wintergreen system

Since the wintergreen-zein systems showed very low particle yields, these systems were considered not to be economically feasible. Therefore the wintergreen oil lost during lyophilisation was not of concern and TGA studies were only performed on the lyophilised wintergreen-to-zein 4:1 system, which showed the highest average particle yield. These results are presented in Figure 4-14 with the results of the pure components.

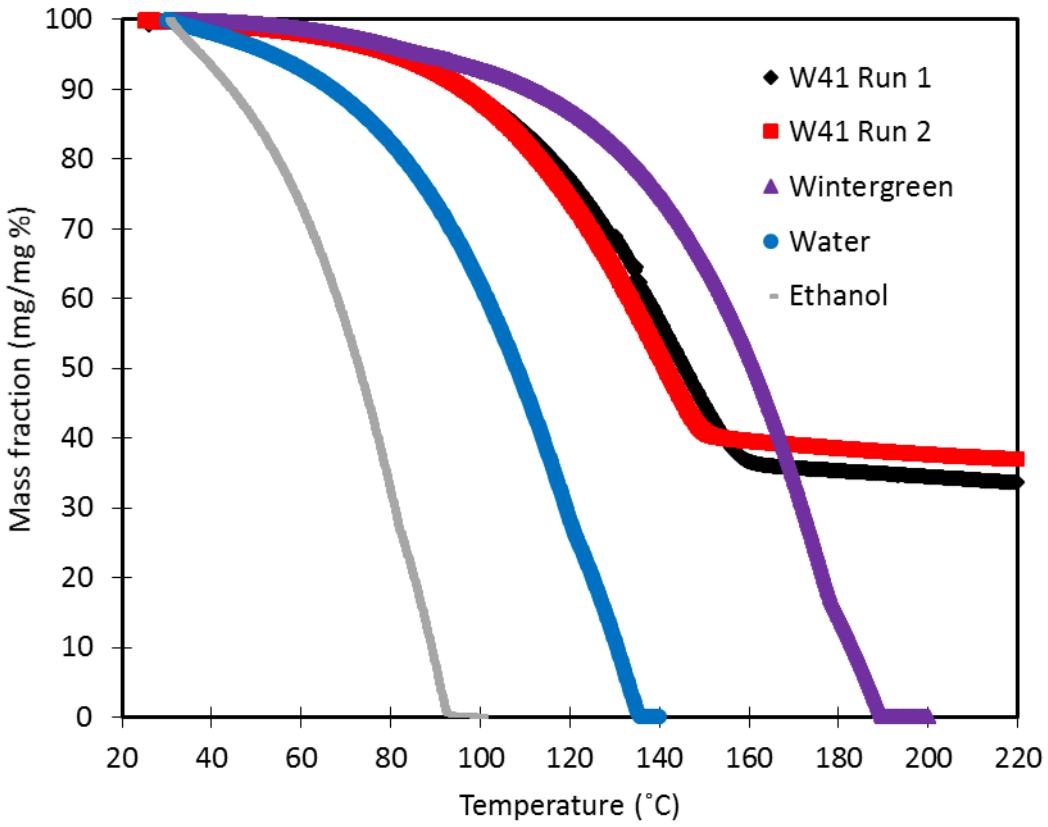


**Figure 4-14: Mass loss of the wintergreen oil-to-zein mass ratio 4:1 micro-particles at different temperatures after lyophilisation**

From Figure 4-14, a significant mass loss of the pure wintergreen commences at approximately 80 ˚C, similarly for the micro-particles where the mass loss onset temperature is higher as it is for the pure water and ethanol.

What it boils down to is that it is reasonable to assume that the observed mass loss of the micro-particles is mainly due to the wintergreen oil. This is a very interesting phenomenon,

i.e. although the wintergreen system showed very poor particle yields, in this case it showed an average wintergreen mass fraction of 66.6%. Therefore, although in totality the interaction between the zein and the wintergreen oil was insignificant, a fraction of the zein may have interacted to such an extent as to encapsulate the wintergreen oil.

The zein participation and wintergreen oil encapsulation efficiencies were calculated to be 28.6% and 14.3% respectively. This shows that some fraction of zein, most probably the more polar fractions, may have participated and the mostly non-polar α-zein to a lesser extent.

## 4.4 Particle size analysis

### 4.4.1 Geraniol-zein systems

The particle size distributions of the geraniol-to-zein mass ratio systems 2:1, 3:1 and 4:1 are shown in Figures 4-15, 4-16 and 4-17 respectively.

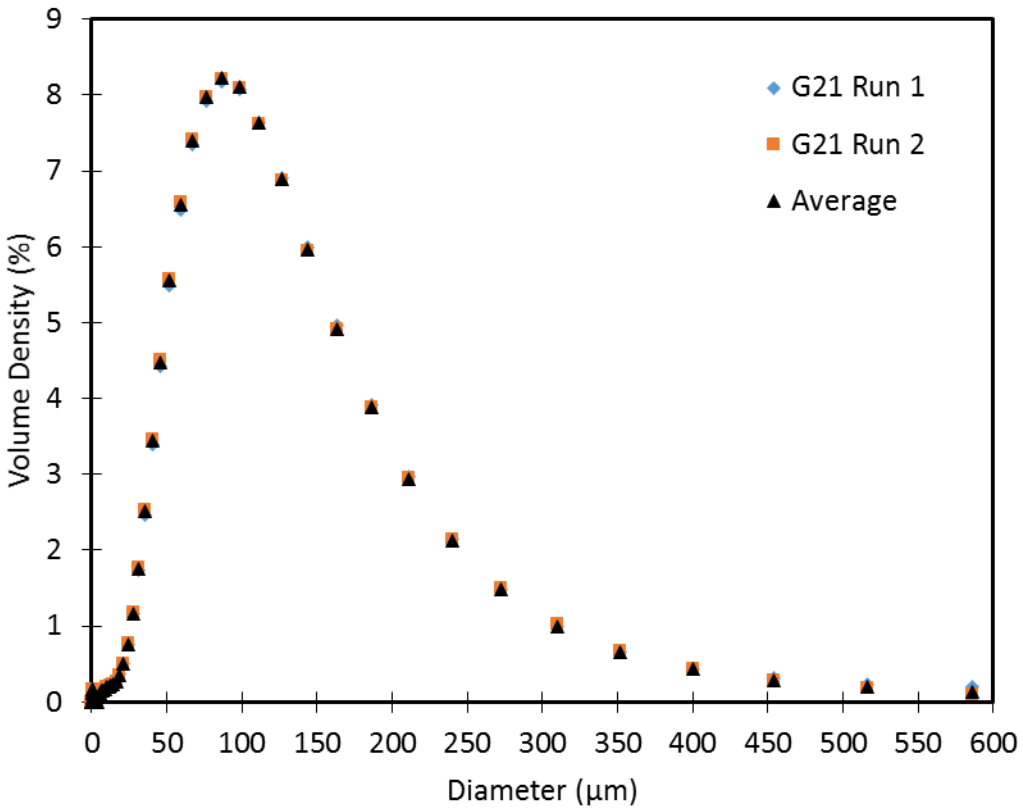


**Figure 4-15: Particle size distribution of the geraniol-to-zein mass ratio 2:1 system.**

From Figure 4-15, the particle size distribution can be seen to be normal, with only one peak, and slightly skew to the smaller particle sizes. The single peak may indicate that there are no distinct differences in the polarity of the zein with which the geraniol interacted, i.e. it suggests that the geraniol only interacted with one fraction of zein, most possibly α-zein. The average D(10) micro-particle size is 40.9 µm, whereas the average D(50) and D(90) equate to 94 µm and 209 µm.

The geraniol-to-zein mass ratio 3:1 system also shows a normal distribution, shown in Figure 4-16, which is skew to the smaller particle sizes. However, the micro-particles are significantly smaller than those of the geraniol-to-zein 2:1 system. The average D(10), D(50) and D(90) particle sizes are only 10.7 µm, 30.5 µm and 86.1 µm respectively.

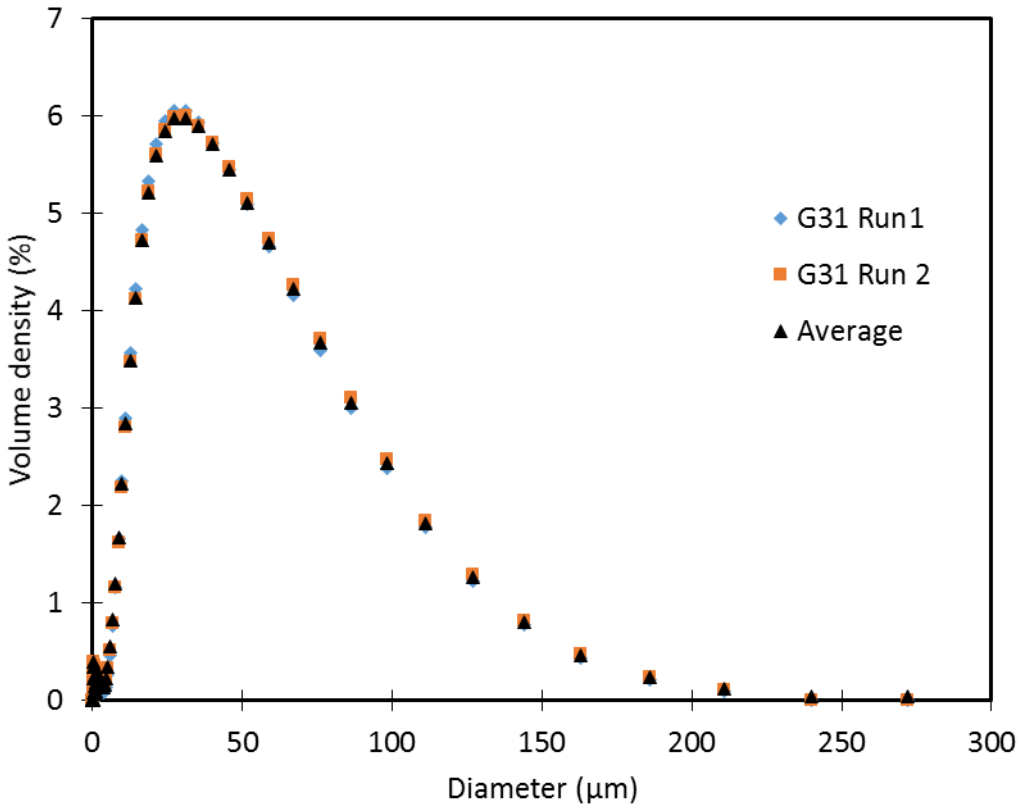


**Figure 4-16: Particle size distribution of the geraniol-to-zein mass ratio 3:1 system.**

Interesting to note is that the size of the micro-particles of the geraniol-to-zein mass ratio 4:1 system, shown in Figure 4-17, is once again bigger than that of the geraniol-to-zein 3:1 system with an average D(10), D(50) and D(90) of 34.3 µm, 95.2 µm and 250 µm respectively.

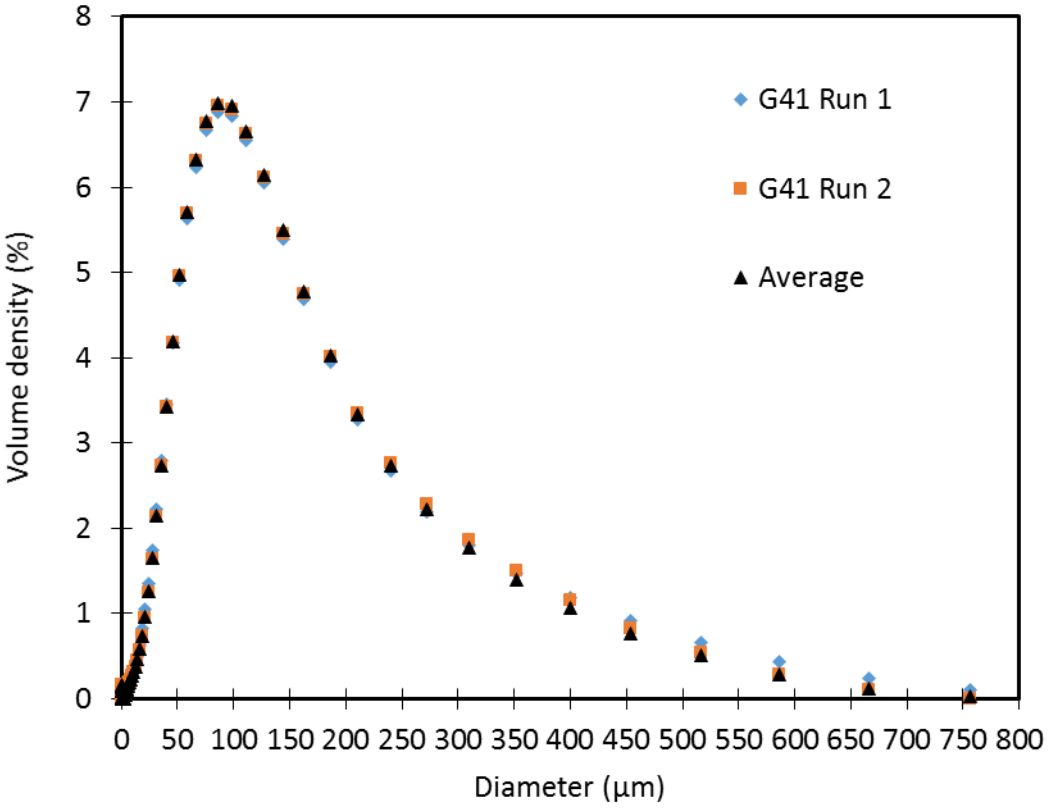


**Figure 4-17: Particle size distribution of the geraniol-to-zein mass ratio 4:1 system.**

An approximation for the wall thickness of a micro-particle for a reservoir system is given by Equation 15.

$$x = \rho_g d/(6\rho_z \xi) \quad (15)$$

Where $x$ is the membrane wall thickness, $\rho_g$ the density of geraniol, $\rho_z$ the density of zein, $d$ the diameter of the microcapsule and $\xi$ the geraniol-to-zein mass ratio of the microcapsule.

The corresponding average values of $\xi$ for the lyophilised geraniol-to-zein mass ratio systems 4:1, 3:1 and 2:1 from the TGA results are 3.7, 2.2 and 1.7. The wall thickness for the D(50) microcapsule of each system can then be estimated to be 3.0 µm, 1.6 µm and 6.5 µm. Clearly, there is a trade-off i.e. the geraniol-to-zein 2:1 system compared to the geraniol-to-zein 4:1 system will have the lowest geraniol content per mass microcapsules, but with the thickest wall membrane, it will have the slowest expected release rate. The geraniol-to-zein 3:1 system, however, will have a moderate geraniol content with the fastest expected

release rate. This is unwanted, but with the highest geraniol encapsulation and zein participation efficiencies it remains the preferred system for study of release kinetics.

### 4.4.2 Wintergreen-zein systems

The average particle size distributions for the best wintergreen systems with the highest particle yields are shown in Figure 4-18.

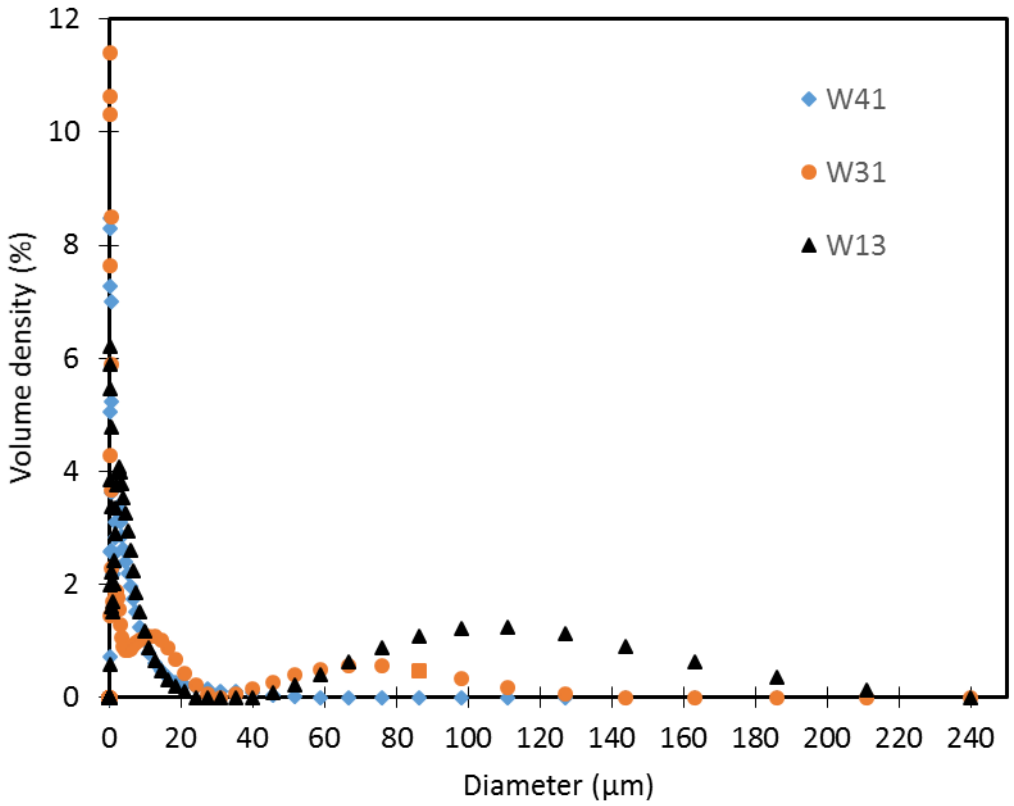


**Figure 4-18: Average particle size distributions of the wintergreen-to-zein mass ratio systems 4:1, 3:1 and 1:3.**

From Figure 4-18 it can be seen that firstly the wintergreen-zein system overall yielded micro-particles with significantly smaller sizes than those encountered in the geraniol-zein systems. Secondly, it also consistently shows three peaks. A possible explanation for this is that it is not just one zein fraction that participated in the formation of these micro-particles. The fractions of zein with the higher polarities should possibly lead to the formation of the micro-particles.

## 4.5 Microscopy

### 4.5.1 Light microscopy

Light microscopy was used for the initial confirmation of the formation of micro-particles. It was also the only method used to visually observe the micro-particles that formed prior to lyophilisation, as the possible presence of non-participating volatiles limited its characterisation with the SEM. An image of multiple micro-particles and a close-up image of one micro-particle of the geraniol-to-zein 3:1 system are shown in Figure 4-19 and Figure 4-20 respectively.

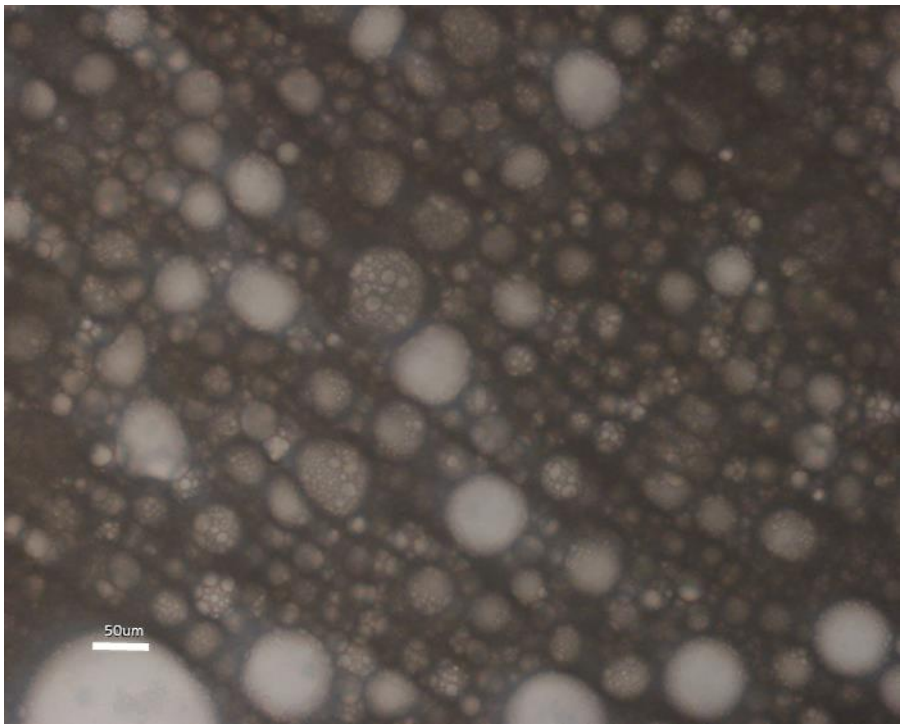


**Figure 4-19: Image of multiple micro-particles of the geraniol-to-zein 3:1 system.**

The first observation is that the size of the micro-particles fall in the vicinity of 50 µm. In addition, their shape appears to be spherical which should reflect in the release kinetics.

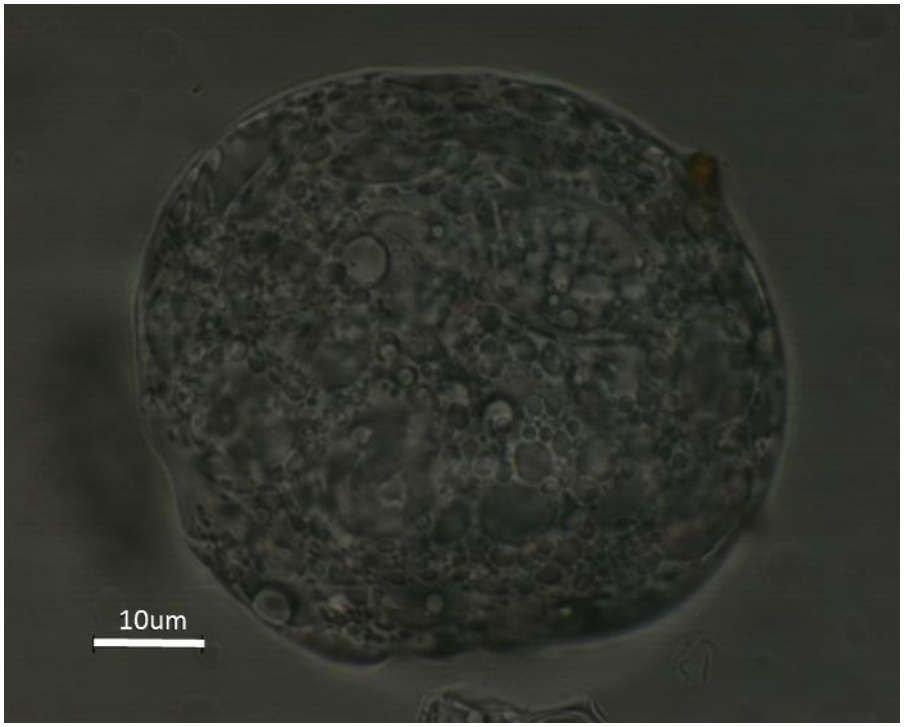


**Figure 4-20: Close-up image of a large micro-particle of the geraniol-to-zein 3:1 system.**

The close-up image in Figure 4-20 reveals that there are roundish irregularities on the surface of the micro-particles. Although it is not clear from this image, the irregularities could either be dents or bumps on the surface. If they are bumps, they can either be bumps within the polymer structure or non-encapsulated surface geraniol adhering to the surface of the zein.

The wintergreen-zein micro-particles, shown in Figure 4-21 and Figure 4-22, also have a spherical shape. These micro-particles are extremely small, with a few exceptionally larger ones (unfortunately they are not in focus due to the size difference) exceeding 10 µm in diameter.

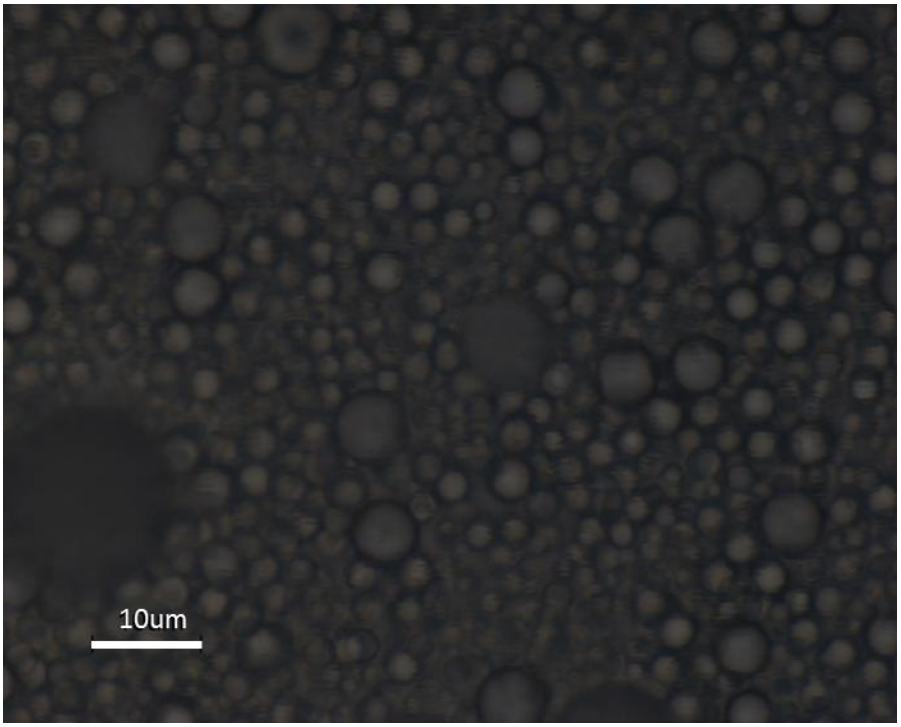


**Figure 4-21: Image of multiple micro-particles of the wintergreen-to-zein 4:1 system.**

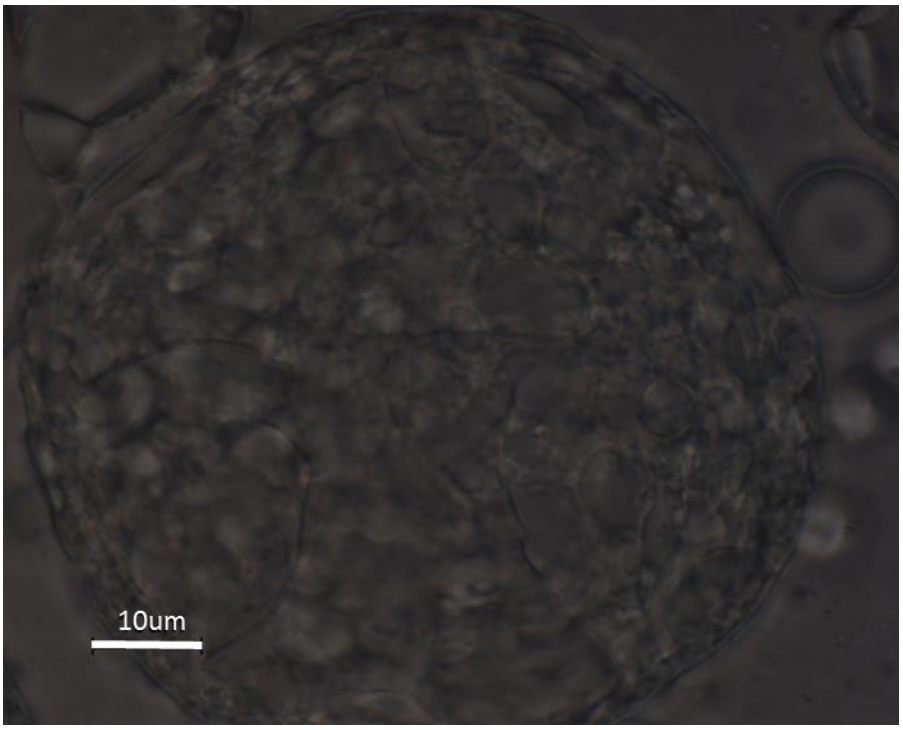


**Figure 4-22: Close-up image of a micro-particle of the wintergreen-to-zein 4:1 system.**

The surface of the wintergreen-zein particle also seems to be irregular; however, the clear spherical geometry of the irregularities is not observed.

### 4.5.2 Scanning electron microscopy

The image of the multiple micro-particles shown in Figure 4-23 shows that the micro-particles retained their spherical geometry after lyophilisation, but they did seem to agglomerate and in some instances formed filament-like structures connecting them. A few ruptured or broken micro-particles were also observed as shown in Figure 4-24 and Figure 4-26, but no collapsed structures were observed.

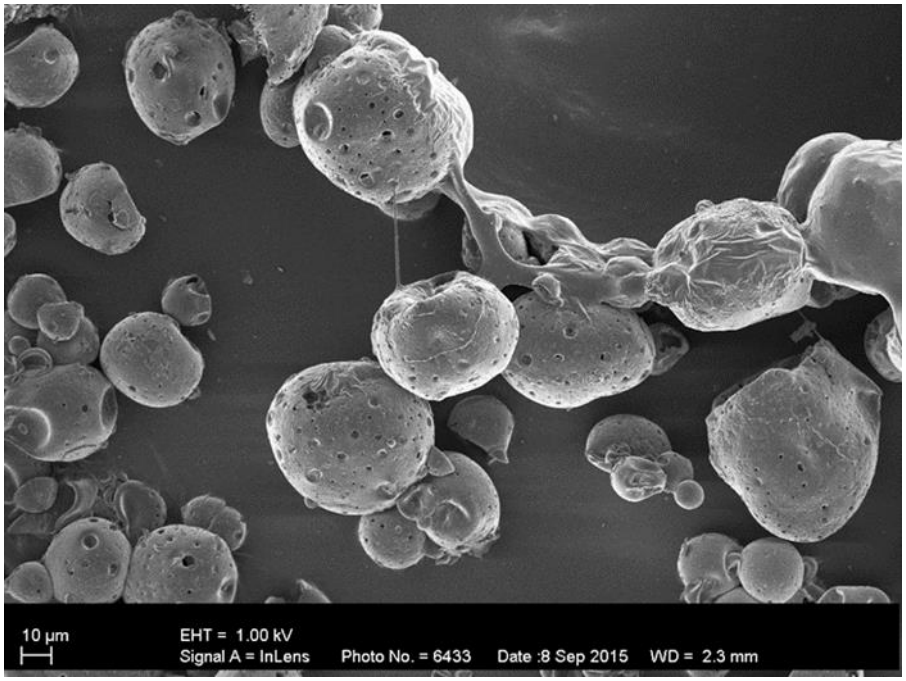


**Figure 4-23: SEM image of multiple micro-particles of the geraniol-to-zein 3:1 system after lyophilisation.**

The ruptured micro-particles showed a view of their internal structure, which revealed that they have a membrane structure with a hollow internal cavity, making them microcapsules. This corresponds to a reservoir system, and possible zero-release kinetics could be observed in their present glassy state. Whether this structure is only limited to the ruptured micro-particles due to the possible collapse of the internal structure upon rupturing, or whether it extends to lyophilised micro-particles, was clarified with confocal microscopy. A close-up image of a micro-particle is shown in Figure 4-25, in which the irregularities on the surface can clearly be seen.

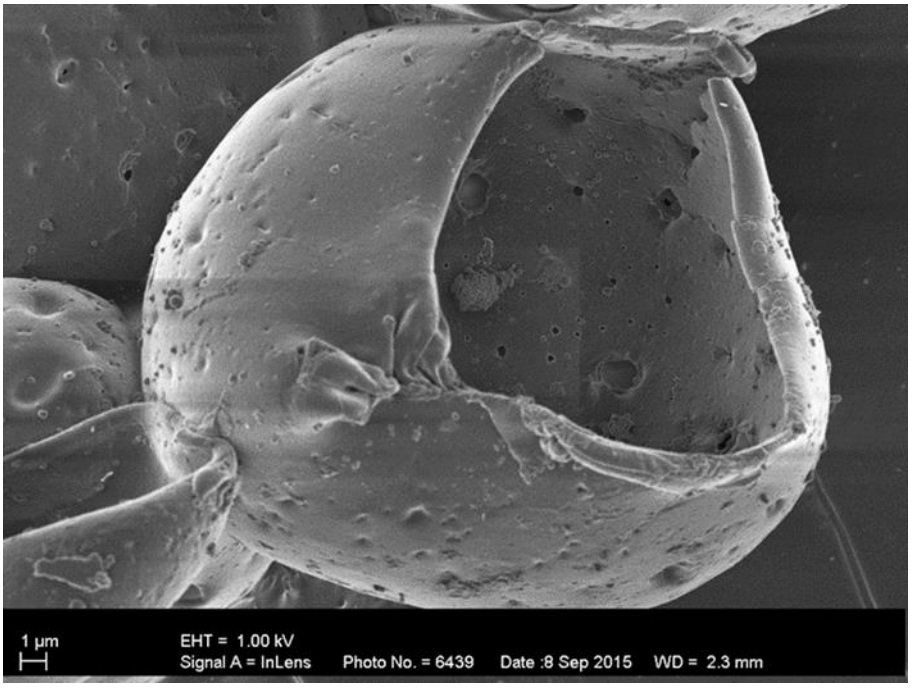


**Figure 4-24: Close-up SEM image of a ruptured micro-particle of the geraniol-to-zein 3:1 system after lyophilisation.**

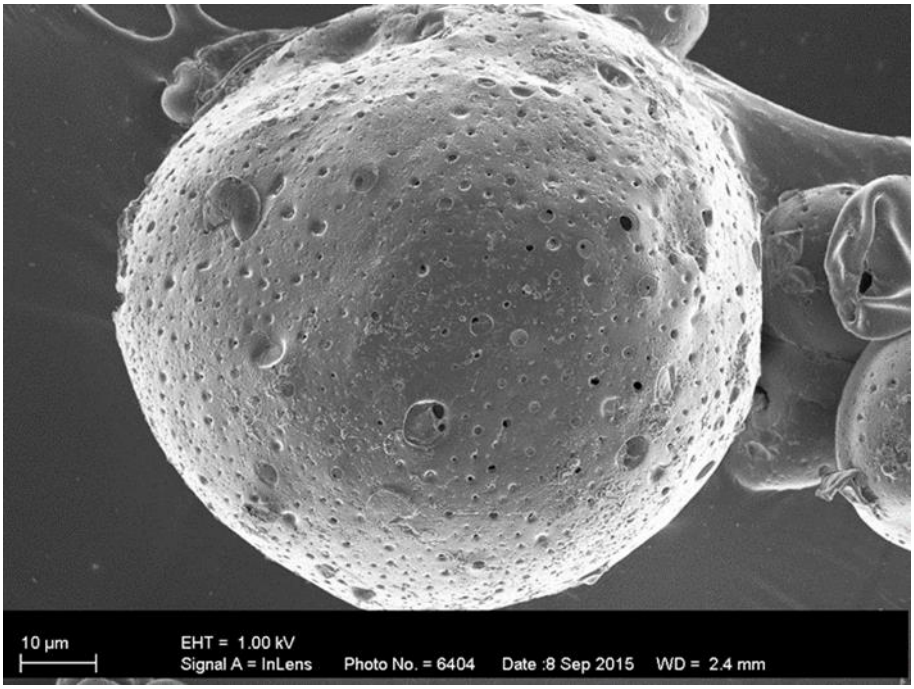


**Figure 4-25: Close-up SEM image of a micro-particle from the geraniol-to-zein 3:1 system after lyophilisation.**

There are definite dents in the polymer structure, with some dents being so severe as to protrude through the membrane exposing the inner cavity. The dents varied between microcapsules observed – the microcapsule shown in Figure 4-26 has a major dent on the

left. The dent on the right may be misleading as it may have been caused by the rupture. Furthermore, from Figure 4-26, the dents protruding through the membrane can be seen from the inside of the microcapsule and the exposed membrane can be observed. A possible explanation for the dents is that non-encapsulated geraniol may have adhered to the surface of the zein and was evaporated during lyophilisation. On closer inspection, in Figure 4-27 the membrane seems to consist of small spherical cavities possibly containing geraniol. In the middle of the membrane it appears that one of these cavities is not closed off to the surface. Therefore the dents observed may be cavities that are not closed off to the surface and the holes may be cavities extending from the inner surface to the outer surface. If the cavities in the membrane contain geraniol, it could have implications for the release kinetics, as a burst effect may be observed when encapsulated oil is present in the membrane of a microcapsule.

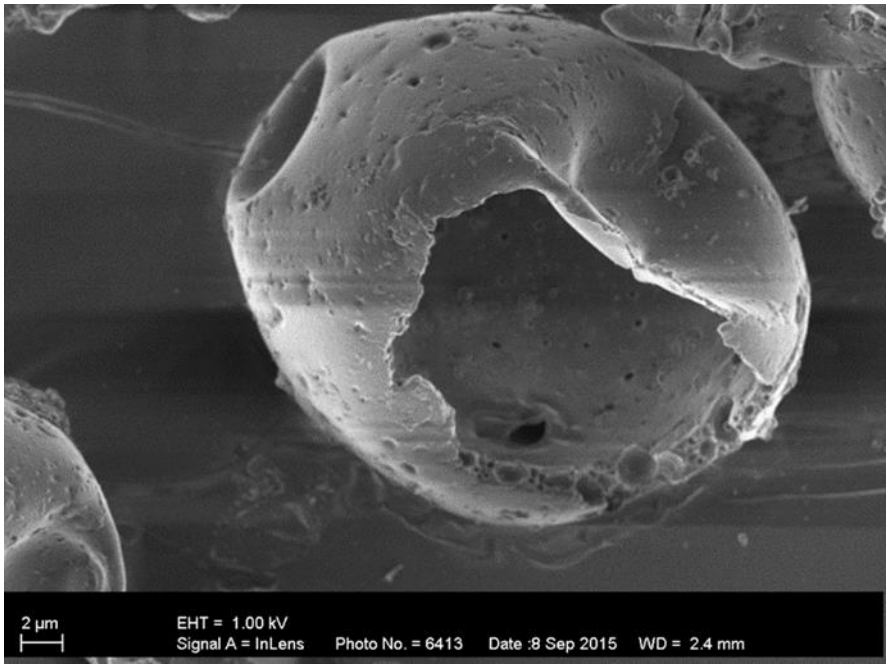


**Figure 4-26: Close-up SEM image of a ruptured micro-particle from the geraniol-to-zein 3:1 system after lyophilisation with exposed membrane**

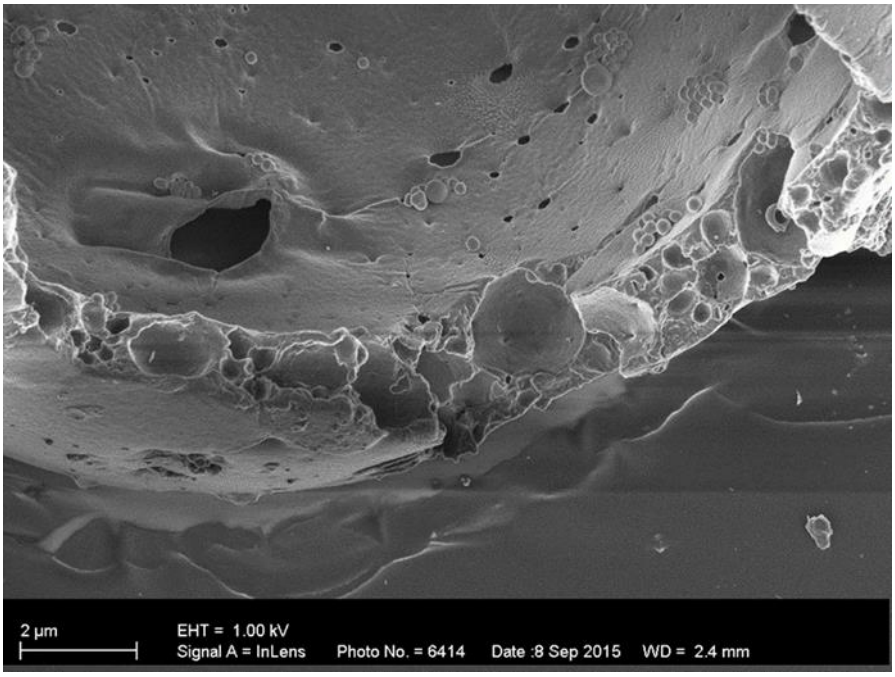


**Figure 4-27: Close-up SEM image of an exposed membrane of a ruptured micro-particle of the geraniol-to-zein 3:1 system after lyophilisation.**

The size of the microcapsule shown in Figure 4-26 and Figure 4-27 is in the range of 30 µm i.e. the D(50) size of the geraniol-to-zein 3:1 system with an approximate membrane thickness (x) of 1.9 µm. This is slightly more than the predicted wall thickness of 1.6 µm indicating that the zein structure is porous, evident from Figure 4-27.

The wintergreen-zein system observed after lyophilisation, as shown in Figure 4-28, showed zein flakes rather than micro-particles.

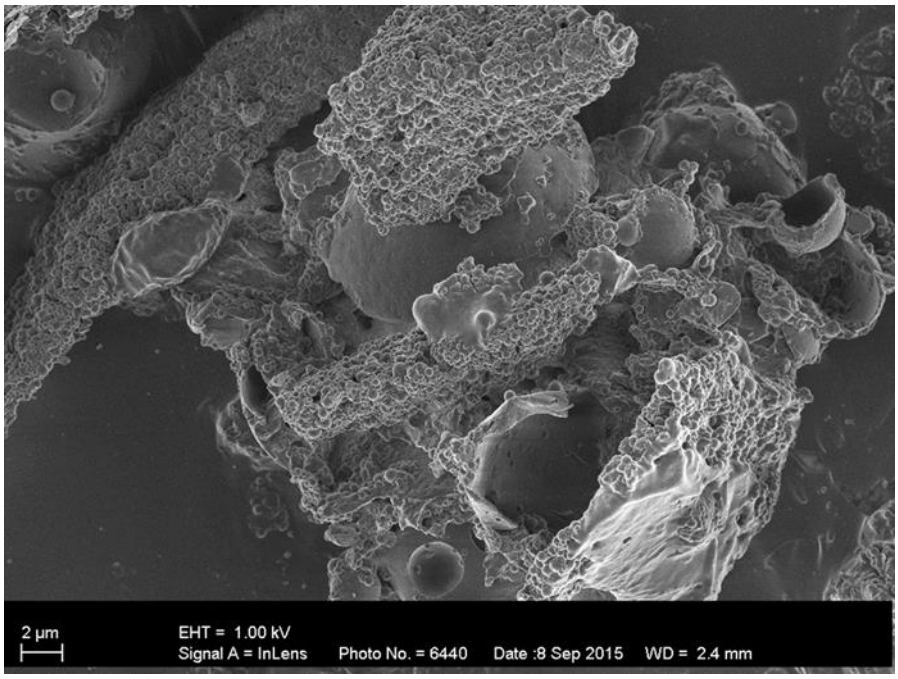


**Figure 4-28: SEM image of zein flakes of the wintergreen-to-zein 4:1 system after lyophilisation.**

Small, spherical objects were also observed on the surface of the flakes. They do not seem to be zein micro-particles themselves, but rather oil droplets. Unfortunately, the reason for the difference in zein structures prior to and after lyophilisation for the wintergreen-zein system is unknown. The low pressure during lyophilisation may have caused the wintergreen to evaporate and the zein micro-particles to burst or collapse.

### 4.5.2 Confocal microscopy

The confocal image of the geraniol-to-zein 3:1 system prior to lyophilisation is shown in Figure 4-29.

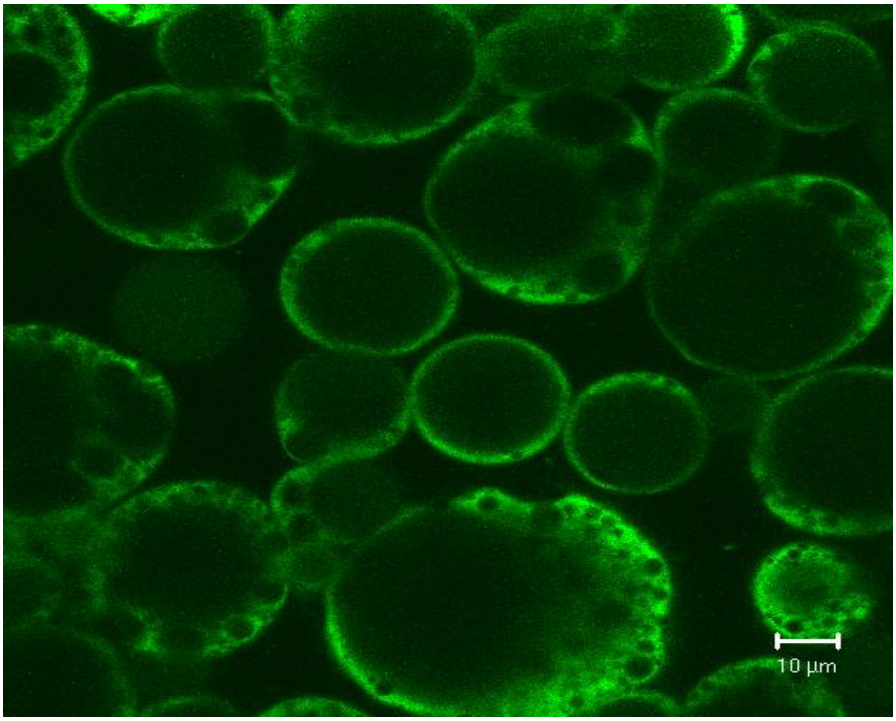


**Figure 4-29: Confocal image of the internal structure of multiple microcapsules of the geraniol-to-zein 3:1 system prior to lyophilisation.**

The internal structures observed in Figure 4-29 corresponds very well to those observed under the SEM. There is a clear, defined core cavity in all the microcapsules, with surrounding smaller cavities in the fluorescing zein membrane wall stained with FITC. The membrane cavities, however, can vary significantly in size between microcapsules. In conclusion, the reservoir system is not only limited to microcapsules that are lyophilised or that have burst, and nearly zero-order kinetics can be expected for the geraniol-to-zein 3:1 system in the glassy and swollen states.

## 4.6 Kinetics

The release kinetics of the geraniol-to-zein 3:1 system at different temperatures is shown in Figure 4-30 as the fraction of oil released.

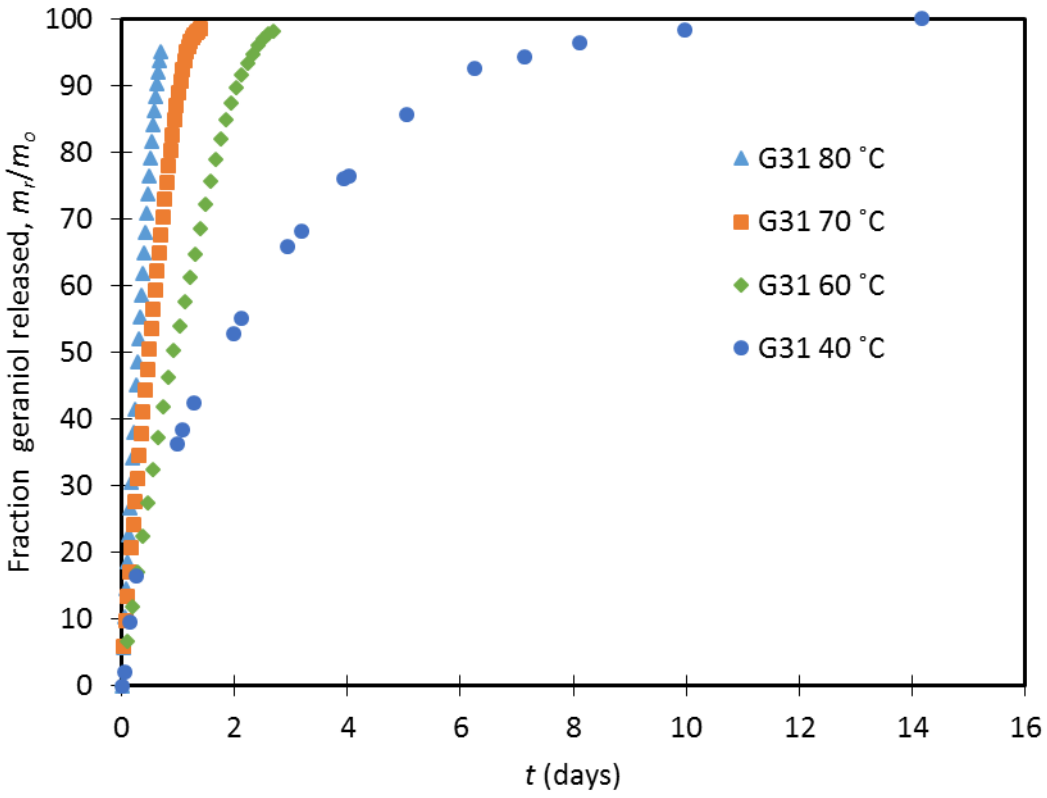


**Figure 4-30: Fraction of encapsulated geraniol released of the geraniol-to-zein 3:1 system at different isothermal temperatures.**

As expected, the geraniol release rate decreases with decreasing temperature. The system exhibits near-linear release behaviour (zero-order kinetics) at all temperatures for geraniol-released values lower than 80%. This behaviour is favourable with regard to the intended application as a constant amount of geraniol is released per unit of time, allowing consistent repellent concentrations. The release kinetics correspond to those of a reservoir system and the conclusions from the SEM and confocal images. However, the linearity seems to weaken as the temperature is decreased, with particular reference to the first 20% of the geraniol released at 40 ˚C. The zoomed-in range is shown in Figure 4-31.

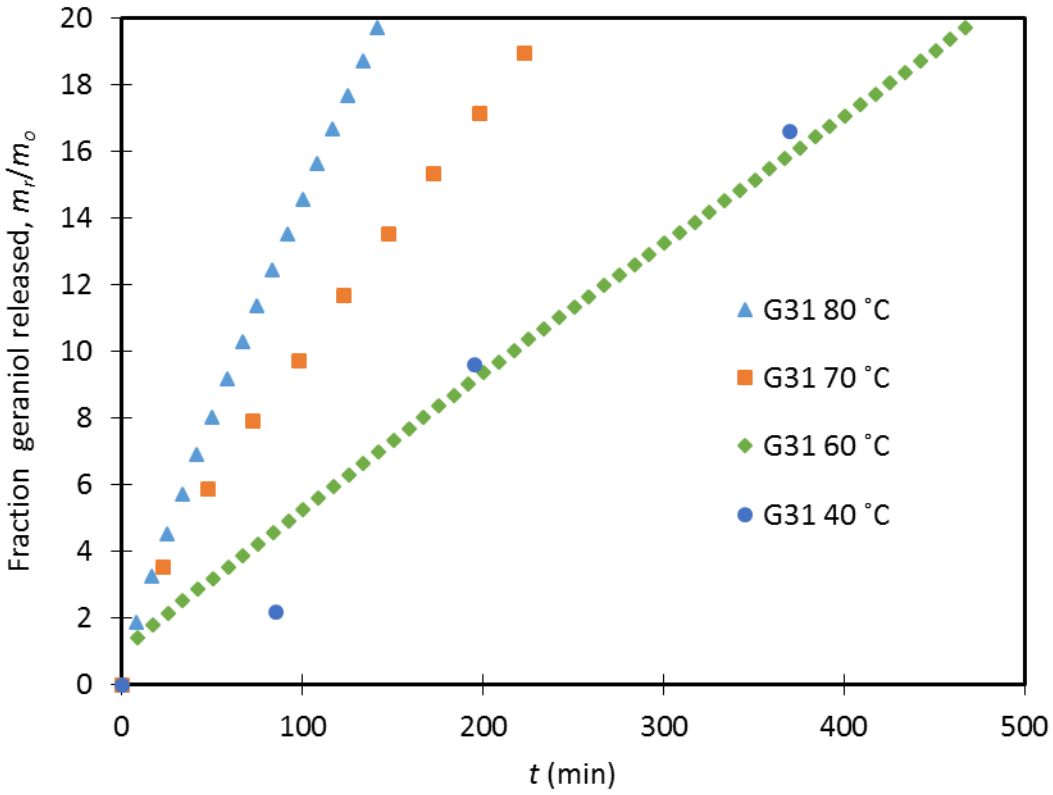


**Figure 4-31: Release kinetics range of the geraniol-to-zein 3:1 system showing non-linearity.**

As can be seen from Figure 4-31, the kinetics at temperatures higher than 40 ˚C also show the non-linearity, but not as profoundly. A possible explanation for this occurrence is the bursting effect, i.e. that the geraniol captured within the membrane wall is initially released at a higher rate (shorter diffusion path) than the bulk of the geraniol in the main reservoir. The combination of the two shows a marked difference from the remaining release profile. At high temperatures, this effect is not as profound as the diffusion from the main reservoir is so high that the additional release from the wall membrane can be regarded as insignificant.

The data were fitted with Equation 4, with the values for n equalling 1 (thin sheet geometry) and 0.85 (spherical geometry) for case II transport from Table 2-6. The values for $k^n$ were then obtained with the least square method. Note that only the data between 20% released and 80% released were taken into account. These values at the respective temperatures are given in Table 4-10. A visual presentation of the mathematical approximations at 60 ˚C, 70 ˚C and 80 ˚C is shown in Figure 4-32.

**Table 4-10: Release kinetics constants at different temperatures for the geraniol-to-zein 3:1 system.**

| Temperature | $k^n$ with n = 1 (1/min) | $k^n$ with n = 0.85 ($1/min^{0.85}$) |
|---|---|---|
| 40 ˚C | 0.000123 | 0.001553 |
| 60 ˚C | 0.000334 | 0.001066 |
| 70 ˚C | 0.000621 | 0.004768 |
| 80 ˚C | 0.001111 | 0.002932 |

In all instances, by taking n = 0.85, a better fit with a smaller cumulative error was obtained. This can also clearly be seen in Figure 4-32. Assuming that the concentration gradient through the wall membrane remains constant, the area of the microcapsules is unaltered and that no morphological changes occur at the different temperatures, then the only variable with temperature will be the diffusivity of the geraniol. Its temperature dependence is given by Equation 16.

$$D = D_o\, e^{-Ea/RT} \qquad (16)$$

Subsequently, $k^n$ will have the same dependency. By taking the natural logarithm on both sides, Equation 17 is obtained.

$$\ln(k^n) = \ln((k_o{}^n) - (nE_a/RT) \qquad (17)$$

The fit to obtain $nE_a/R$ is shown in Figure 4-33.

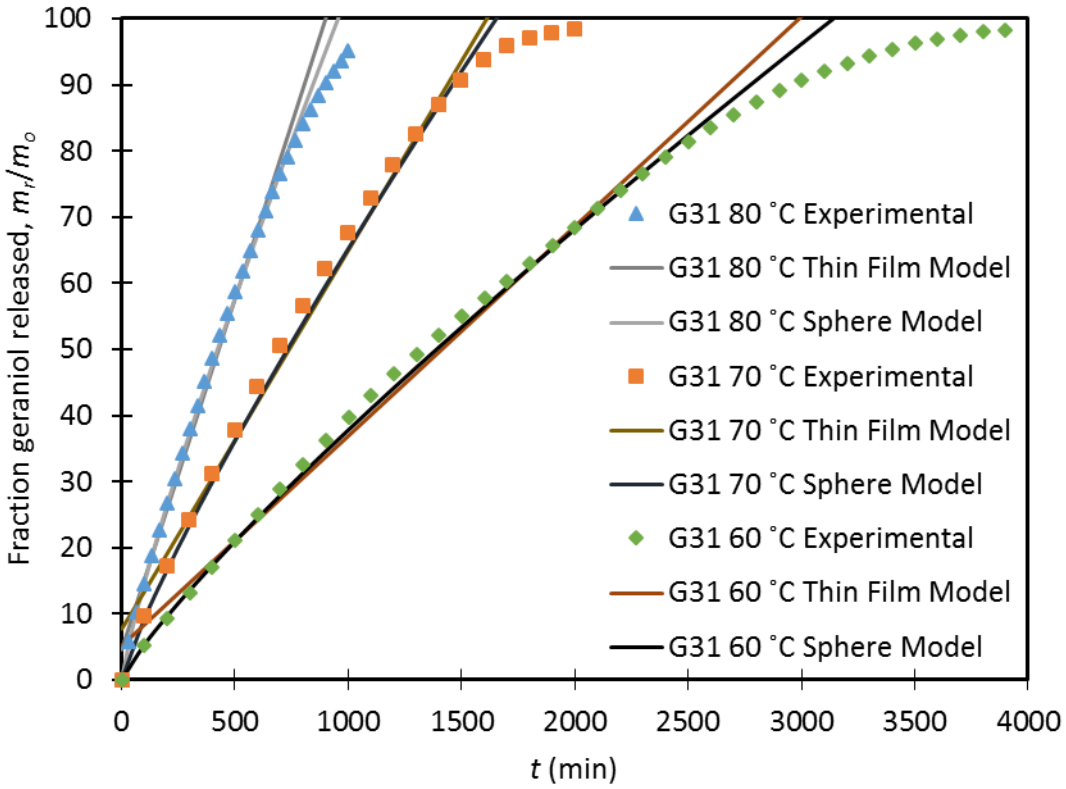


**Figure 4-32: Mathematical approximations of release rate for the thin film and spherical geometries at 60 ˚C, 70 ˚C and 80 ˚C of the geraniol-to-zein 3:1 system.**

The data showed a very good linear trend and the values for n$E_a$/R were fitted to be 6048.9 K and 5033.2 K for the thin film and spherical geometry approximations respectively.

Consequently, the time needed for the microcapsules to release 80% of their initial geraniol content at 20 ˚C and 30 ˚C could be predicted as 25 342 min and 12 863 min respectively using the linear model, and 20976 min and 11 114 min respectively using the sphere model. In terms of days where one day equals 24 hours, the corresponding values are 17.6, 8.9, 14.6 and 7.7 days.

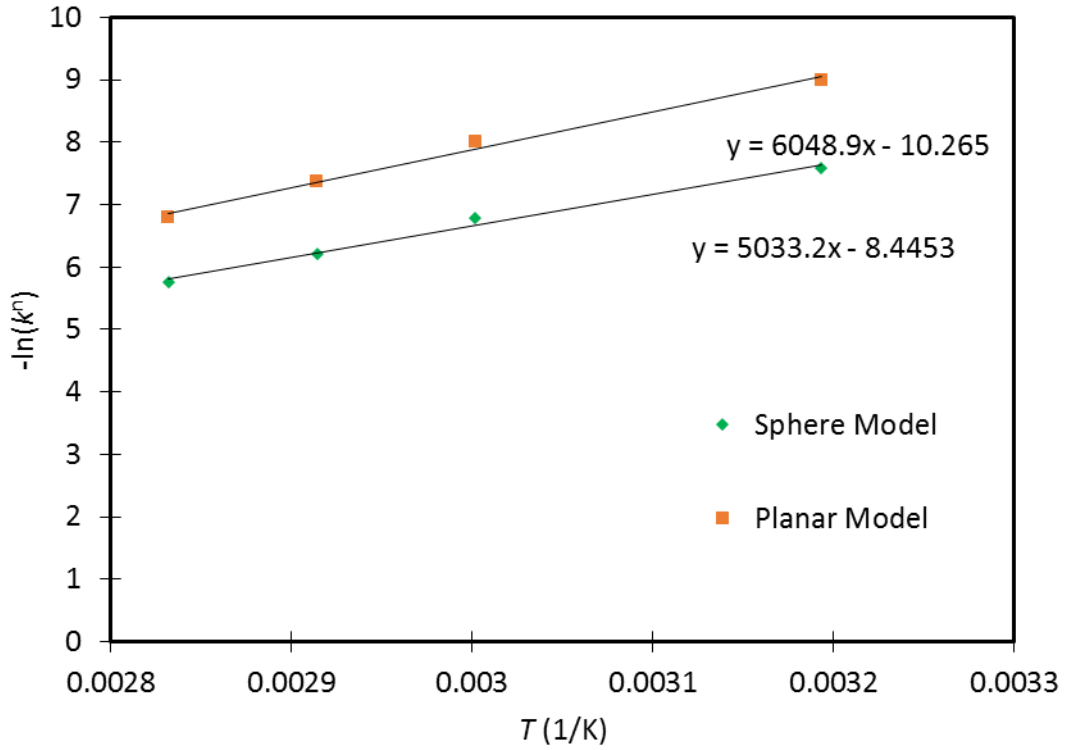


**Figure 4-33: Value of -ln($k^n$) at different temperatures with trend lines.**

# 5 Conclusions and Recommendations

The conclusions for the geraniol-zein system are:

- At geraniol-to-zein mass ratios of 1:1 and lower, practically no microcapsules were formed, but at geraniol-to-zein mass ratios of 2:1 and higher, particle yields of up to 85% were observed. Proposed explanations for this phenomenon include a micellar inversion of zein at geraniol-to-zein mass ratios greater than unity due to an increase in the hydrophobicity of the environment or higher phase separation kinetics at these geraniol-to-zein mass ratios. This may cause the geraniol to phase separate first, be emulsified by continued stirring and followed by the zein, enabling encapsulation.
- The geraniol mass fraction increased with higher geraniol content. Of the geraniol-to-zein mass ratios investigated, the geraniol-to-zein 4:1 system showed the highest geraniol mass fraction. However, the geraniol-to-zein 3:1 system showed the best utilisation of materials with the highest geraniol encapsulation and zein participation efficiencies. From this it was concluded that the geraniol-to-zein 3:1 system might be the most economically viable for large-scale agricultural use.
- In all cases, the thermodynamic modelling approach predicted a worst case scenario in terms of estimating the fraction of geraniol lost during lyophilisation. The geraniol-to-zein 3:1 system showed the highest loss at 8.2%.
- During particle size analysis a single peak was consistently observed. The geraniol-to-zein 3:1 system differed from the other systems as it is comprised of much smaller microcapsules. This corresponded to the higher geraniol encapsulation and zein participation efficiencies.
- Light microscopy revealed that the microcapsules were spherical in shape with irregular surfaces prior to lyophilisation. SEM indicated that there were dents on the surface of the microcapsules, which could possibly be areas to which non-encapsulated geraniol adhered. SEM and confocal microscopy showed that the microcapsules had large central cavities with a surrounding zein membrane. This classified the microcapsules as reservoir systems. Smaller cavities were also observed within the membrane wall.

- Release kinetics of the geraniol-to-zein 3:1 system approximated zero-order characteristics. This corresponds to a glassy polymer reservoir system. Some non-linearity in the initial release profile was observed. This is possibly a small bursting effect caused by the geraniol in the cavities within the zein membrane. Extrapolation of release constants at different temperatures showed that the time period for the geraniol-to-zein 3:1 system to release 80% of the initial geraniol content can range from 7.7 and 17.6 days at 20 ˚C and 30 ˚C respectively.

The conclusions for the wintergreen oil-zein system are:

- The wintergreen-zein system showed very low, inconsistent particle yields compared to the geraniol-zein system, but showed significant wintergreen oil mass fractions. A possible reason for the low particle yields is the high polarity of the major constituent of wintergreen oil, methyl salicylate. This may not favour encapsulation by the predominantly hydrophobic zein.
- Particle size analysis showed several peaks, possibly indicating differing extents of interaction by different zein fractions.
- Light microscopy revealed that these micro-particles were also spherical in shape prior to lyophilisation, but the SEM images showed the zein to be flakes after lyophilisation with possible wintergreen oil droplets adhering to them.

Recommendations for future investigations are to:

- Extend the range of geraniol/wintergreen oil-to-zein mass ratios beyond those studied in this study.
- Establish the initial zein fraction content by selective solubility.
- Establish the zein fraction content that participated in the encapsulation of geraniol and wintergreen by selective solubility.
- Experimentally determine the orientation of the moieties of zein micelles at different geraniol contents by studying their interaction with polar and non-polar surfaces.
- Study the kinetics of the phase separation of geraniol and zein e.g. by varying the rate at which additional water is added.

- Establish the effect that different stirrer speeds will have on the geometry and microcapsule size.
- Study the swelling and release kinetics of the geraniol-zein system in an aqueous environment to determine whether swelling takes place, and if so, how it will affect the release profile. This is for the possible distribution of the microcapsules in irrigation systems.
- Explore methods of blending diffusion-inhibiting materials with zein to extend the release period of the geraniol.
- Explore more polar biopolymers for the encapsulation of wintergreen oil.
- Study the rheology of the microcapsules to determine at which shear rates the microcapsules will be mechanically damaged, for the purpose of establishing flow rates in irrigation systems.
- Determine the effectiveness of the microcapsules as an aphid repellent by means of olfactory studies, especially in a South African context.

# References

*CID=4133* [Online]. PubChem Compound Database: National Center for Biotechnology Information. Available: https://pubchem.ncbi.nlm.nih.gov/compound/4133 [Accessed 29 October 2015].

*CID=637566* [Online]. PubChem Compound Database: National Center for Biotechnology Information. Available: https://pubchem.ncbi.nlm.nih.gov/compound/637566 [Accessed 28 October 2015].

*GPS Safety Summary Geraniol* [Online]. Available: http://product-finder.basf.com/group/corporate/product-finder/en/literature-document:/GPS+Safety+Summaries--Geraniol-English.pdf [Accessed 1 November 2015].

*Hydrocarbons* [Online]. Purdue University. Available: http://chemed.chem.purdue.edu/genchem/topicreview/bp/1organic/hydro.html [Accessed 29 October 2015].

ALLSOPP, E., PRINSLOO, G. J., SMART, L. E. & DEWHIRST, S. Y. 2014. Methyl salicylate, thymol and carvacrol as oviposition deterrents for Frankliniella occidentalis (Pergande) on plum blossoms. *Anthropod-Plant Interactions,* 8**,** 421-427.

AMENT, K., KANT, M. R., SABELIS, M. W., HARING, M. A. & SCHUURINK, R. C. 2004. Jasmonic acid is a key regulator of spider mite-induced volatile terpenoid and methyl salicylate emission in tomato. *Plant Physiol.,* 135**,** 2025-2037.

ANAL, A. K. & SINGH, H. 2007. Recent advances in microencapsulation of probiotics for industrial applications and targeted delivery. *Trends in Food Science & Technology,* 18**,** 240-251.

ARGOS, P., PEDERSEN, K., MARKS, M. D. & LARKINS, B. A. 1982. A structural model for maize zein proteins. *J. Biol. Chem.,* 257**,** 9984-9990.

ARIMURA, G., OZAWA, R., NISHIOKA, T., BOLAND, W., KOCH, T., KUHNEMANN, F. & TAKABAYASHI, J. 2002. Herbivore-induced volatiles induce emission of ethylene in neighboring lima bean plants. *Plant J***,** 87-98.

BAKKALI, F., AVERBECK, S., AVERBECK, D. & IDAOMAR, I. 2008. Biological effects of essential oils-A review. *Food and Chemical Toxicology,* 46**,** 446-475.

## References

BAŞER, K. H. C., KÜRKCÜOGLU, M. & DEMIRCI, B. 2005. Ninde oil (Aeollanthus myrianthus Taylor) revisited: analysis of a historical oil. *Journal of Essential Oil Research,* 17**,** 137-138.

BAYDAR, H. & BAYDAR, N. G. 2005. The effects of harvest date, fermentation duration and Tween 20 treatment on essential oil content and composition of industrial oil rose (Rosa damascena Mill.). *Industrial Crops and Products,* 21**,** 251-255.

BERNASCONI, M. L., TURLINGS, T. C. J., AMBROSETTI, L., BASSETTI, P. & DORN, S. 1998. Herbivore-induced emissions of maize volatiles repel the corn leaf aphid, *Rhopalosiphum maidis*. *Entomologia Experimentalis et Applicata,* 87**,** 133-142.

BLACKMAN, R. L. 1974. *Aphids,* London, Ginn & Company Limited.

BLACKMAN, R. L. & EASTOP, V. F. 2000. *Aphids on the Worlds Crops,* Chichester, Wiley.

BRINKHUIS, R. P., RUTJES, F. P. J. T. & VAN HEST, C. C. M. 2011. Polymeric vesicles in biomedical applications. *Polymeric Chemistry,* 2**,** 1449-1462.

CHEN, W. & VILJOEN, A. M. 2010. Geraniol — A review of a commercially important fragrance material. *South African Journal of Botany,* 76**,** 643-651.

CRAINE, E. M., FREIMUTH, D. V., BOUNDY, J. A. & DIMLER, R. J. 1961. Preparation of purified zein by adsorption-desorption. *Cereal Chem.,* 38**,** 399-407.

DANZER, L. A., ADES, H. & REES, E. D. 1975. The helical content of zein, a water insoluble protein, in non-aqueous solvents. *Biochim. Biophys.,* 386**,** 26-31.

DEWHIRST, S. Y., PICKETT, J. A. & HARDIE, J. 2010. Chapter Twenty-Two - Aphid Pheromones. *In:* GERALD, L. (ed.) *Vitamins & Hormones.* Academic Press.

DUBEY, V. S. & LUTHRA, R. 2001. Biotransformation of geranyl acetate to geraniol during palmarosa (Cymbopogon martinii, Roxb. wats. var. motia) inflorescence development. *Phytochemistry,* 57**,** 675-680.

ESEN, A. 1986. Separation of alcohol-soluble proteins (zeins) from maize into three fractions by differential solubility. *Plant Physiol.,* 80**,** 623-627.

ESEN, A. 1987. A proposed nomenclature for alcohol-soluble proteins (zeins) of maize (*Zea mays* L.). *J. Cereal Sci.,* 5**,** 117-128.

EVANS, C. & MANLEY, R. H. 1941. Solvents for zein. *Ind. Eng. Chem.,* 33**,** 1416-1417.

EVANS, C. D. & MANLEY, R. H. 1944. Ternary solvents for zein. *Ind. Eng. Chem.,* 36.

FACCIOLA, S. 1998. *Cornucopia II: A Source Book of Edible Plants,* UK, Kampong Publications.

**References**

FAN, J., ZHANG, Y., FRANCIS, F., CHENG, D., SUN, J. & CHEN, J. 2015. Orco mediates olfactory behaviors and winged morph differentiation induced by alarm pheromone in the grain aphid, Sitobion avenae. *Insect Biochemistry and Molecular Biology,* 64**,** 16-24.

FANG, A. & CATHALA, B. 2010. Smart swelling biopolymer microparticles by a microfluidic approach: Synthesis, *in situ* encapsulation and controlled release. *Colloids and Surfaces B: Biointerfaces,* 82**,** 81-86.

GIANAZZA, E., VIGLIENGHI, V., RIGHETTI, P. G., SALAMINI, F. & SOAVE, C. 1977. Amino acid composition of zein molecular components. *Phytochemistry,* 16**,** 315-317.

GORTNER, R. A. & MACDONALD, R. T. 1944. Studies on the fractionation of zein. *Cereal Chem.,* 21**,** 324-333.

GURUNG, K. 2007. Analysis of Wintergreen Oil Extracted from Leaves of Wintergreen in Distillation Units of Dolakha. Dolakha Nepal: Ecology Agriculture and Rural Development Society.

HALBERT, S. E., CORSINI, D., WIEBE, M. & VAUGHN, S. F. 2008. Plant-derived compounds and extracts with potential as aphid repellents. *Annals of Applied Biology,* 154**,** 303-307.

HARDIE, J., ISAACS, R., PICKETT, J. A., WADHAMS, L. J. & WOODCOCK, C. M. 1994. Methyl salicylate and (−)-(1R,5S)-myrtenal are plant-derived repellents for black bean aphid, *Aphis fabae* Scop. (Homoptera: Aphididae). *Journal of Chemical Ecology,* 20**,** 2847-2855.

HELLER, J. & HOFFMAN, A. S. 2004. Drug Delivery Systems. *In:* RATNER, B. D., HOFFMAN, A. S., SCHOEN, F. J. & LEMONS, J. E. (eds.) *Biomaterials Science - An Introduction to Materials in Medicine.* 2nd ed.: Elsevier.

HIGUCHI, T. 1961. Rate of release of medicaments from ointment bases containing drugs in suspensions. *J. Pharm. Sci.,* 50**,** 874-875.

JEON, J. H., LEE, C. H. & LEE, H. S. 2009. Food protective effect of geraniol and its congeners against stored food mites. *Journal of Food Protection,* 72**,** 1468-1471.

JUNG, J. & PERRUT, M. 2001. Particle design using supercritical fluids: Literature and patent survey. *Journal of Supercritical Fluids,,* 20**,** 179-219.

KIM, S. & XU, J. 2008. Aggregate formation of zein and its structural inversion in aqueous ethanol. *Journal of Cereal Science,* 47**,** 1-5.

KOUL, O., WALIA, S. & DHALIWAL, G. S. 2008. Essential Oils as Green Pesticides: Potential and Constraints. *Biopesticides International,* 4**,** 63-84.

LAPCZYNSKI, A., JONES, L., MCGINTY, D., BHATIA, S. P., LETIZIA, C. S. & API, A. M. 2007. Fragrance material review on methyl salicylate. *Food and Chemical Toxicology,* 45**,** S428-S452.

LIDE, D. 2004. *CRC Handbook of Chemistry and Physics*, CRC Press.

LIU, X., SUN, Q., WANG, H., ZHANG, L. & WANG, J.-Y. 2005. Microspheres of corn protein, zein, for an ivermectin drug delivery system. *Biomaterials,* 26**,** 109-115.

MATSUSHIMA, N., DANNO, G., TAKEZAWA, H. & IZUMI, Y. 1993. Three dimensional structure of maize α-zein proteins studied by small angle X-ray scattering. *Biophys,* 1339.

MOSSÉ, J. 1961. Monographie sur une prote´ine du mais: la ze´ine. *Ann. Physiol. Ve´g.,* 3**,** 105-139.

MÜLLER, G. C., JUNNILA, A., KRAVCHENKO, V. D., REVAY, E. E., BUTLER, J. & SCHLEIN, Y. 2008. Indoor protection against mosquito and sand fly bites: a comparison between citronella, linalool, and geraniol candles. *Journal of the American Mosquito Control Association,* 24**,** 150-153.

NAULT, L. R. 1997. Arthropod transmission of plant viruses: A new synthesis. *Ann. Entomol. Soc. Am.,* 90**,** 521-541.

NIE, Z., XU, S., SEO, M., LEWIS, P. C. & KUMACHEVA, E. 2005. *J. Am. Chem. Soc.,* 127**,** 8058.

NIKOLIĆ, M., MARKOVIĆ, T., MOJOVIĆ, M., PEJIN, B., SAVIĆ, A., PERIĆ, T., MARKOVIĆ, D., STEVIĆ, T. & SOKOVIĆ, M. 2013. Chemical composition and biological activity of Gaultheria procumbens L. essential oil. *Industrial Crops and Products,* 49**,** 561-567.

OKUSHIMA, T., NISISAKO, T., TORII, T. & HIGUCHI, T. 2004. *Langmuir***,** 9905.

OMOLO, M. O., OKINYO, D., NDIEGE, I. O., LWANDE, W. & HASSANALI, A. 2004. Repellency of essential oils of some Kenyan plants against *Anopheles gambiae*. *Phytochemistry,* 65**,** 2797-2802.

ONWULATA, C. I. & HUTH, P. J. 2009. Whey Protein Hydrogels and Nanoparticles for Encapsulation and Controlled Delivery. *In:* ONWULATA, C. I. & HUTH, P. J. (eds.) *Whey Processing, Functionality and Health Benefits.* Wiley.

PARÉ, P. W. & TUMLINSON, J. H. 1999. Plant Volatiles as a Defense against Insect Herbivores. *Plant Physiology,* 121**,** 325-331.

PARK, T. G., LU, W. Q. & CROTTS, G. 1995. Importance of in vitro experimental conditions on protein release kinetics, stability and polymer degradation in protein encapsulated poly(D,L-lactic acid-coglycolic acid) microspheres. *J Control Release,* 33**,** 211-222.

PETERSSON, J., PICKETT, J. A., PYE, B. J., QUIROZ, A., SMART, L. E., WADHAMS, L. J. & WOODCOCK, C. M. 1994. Winter host component reduces colonization by bird-cherry-oat aphid, Rhopalosiphum padi (L.) (Homoptera, Aphididae), and other aphids in cereal fields. *Journal of Chemical Ecology,* 20**,** 2565-2574.

POMES, A. F. 1971. Zein. In. *In:* MARK, H. (ed.) *Encyclopedia of Polymer Science and Technology.* New York: Wiley.

QUISPE-CONDORI, S., SALDAÑA, M. D. A. & TEMELLI, F. 2011. Microencapsulation of flax oil with zein using spray and freeze drying. *LWT - Food Science and Technology,* 44**,** 1880-1887.

RAJESWARA RAO, B. R., BHATTACHARYA, A. K., MALLAVARAPU, G. R. & RAMESH, S. 2004. Yellowing and crinkling disease and its impact on the yield and composition of the essential oil of citronella (Cymbopogon winterianus Jowitt.). *Flavour and Fragrance Journal,* 19**,** 344-350.

REDDING, B. K. J. 1990. *Microencapsulated pesticides with a lure*.

RICCI, M., PADIN, S., RINGUELET, J. & KAHAN, A. 2006. Use of lemongrass (*Cymbopogon citratus* Stapf.)essential oil as a repellent of *Diuraphis noxia* Kurdj. (Hemiptera: Aphididae) in wheat. *Agricultura Técnica,* 66**,** 256-263.

RITGER, P. L. & PEPPAS, N. A. 1987. A simple equation for description of solute release II. Fickian and anomalous release from swellable devices. *Journal of Controlled Release,* 5**,** 37-42.

SHUKLA, R. & CHERYAN, M. 2001. Zein: the industrial protein from corn. *Industrial Crops and Products,* 13**,** 171-192.

SIEGEL, R. A. & RATHBONE, M. J. 2012. Overview of Controlled Release Mechanisms. *In:* SIEPMANN, J., SIEGEL, R. A. & RATHBONE, M. J. (eds.) *Fundamentals and Applications of Controlled Release Drug Delivery.* Springer US.

SIEPMANN, J. & PEPPAS, N. A. 2001. Modeling of drug release from delivery systems based on hydroxypropyl methylcellulose (HPMC). *Advanced Drug Delivery Reviews,* 48**,** 139-157.

WANG, Q., GEIL, P. H. & PADUA, G. W. 2004b. Role of hydrophilic and hydrophobic interactions in structure development of zein films. *Journal of Polymers and the Environment,* 12**,** 197-202.

WANG, Q., WANG, J. F., GEIL, P. H. & PADUA, G. W. 2004a. Zein adsorption to hydrophilic and hydrophobic surfaces investigated by surface plasmon resonance. *Biomacromolecules,* 5**,** 1356-1361.

WATSON, C. C., ARRHENIUS, S. & WILLIAM, J. W. 1936. Physical chemistry of zein. *Nature,* 137**,** 322-323.

WATSON, S. A. & RAMSTAD, P. E. 1987. *Corn: Chemistry and Technology*, American Association of Cereal Chemists.

WU, X. S. 1995. Preparation, characterization, and drug delivery applications of microspheres based on biodegradable lactic: glycolic acid polymers. *In:* WISE, D. L., TRANTOLO, D. J., ALTOBELLI, D. E., YASZEMSKI, M. J., GRESSER, J. D. & SCHWARTZ, E. R. (eds.) *Encyclopedic handbook of biomaterials and bioengineering. Part A: materials.* New York: Marcel Dekker.

YAWS, C. L., NARASIMHAN, P. K. & GABBULA, C. 2005. *Yaws' Handbook of Antoine Coefficients for Vapor Pressure (2nd Electronic Edition)*, Knovel.

ZHONG, Q., JIN, M., DAVIDSON, P. M. & ZIVANOVIC, S. 2009. Sustained release of lysozyme from zein microcapsules produced by a supercritical anti-solvent process. *Food Chemistry,* 115**,** 697-700.

ZHU, J. & PARK, K. C. 2005. Methyl salicylate, a soybean aphid-induced plant volatile attractive to the predator Coccinella septempunctata. *J. Chem. Ecol. ,* 31**,** 1733-1746.

# Appendix I

The method for the mathematical approximation of the TGA vapour compositions and subsequent calculated encapsulation efficiencies and the geraniol and zein participation efficiencies are explained in this section.

The vapour pressures of the ethanol, water and geraniol were calculated using the Antoine equation represented by Equation 1, which is repeated here for convenience.

$$\log P(T) = A_k - B\,(T+C) \qquad (1)$$

The values for the constants $A_k$, B and C, as well as the units for the vapour pressure ($P_i$) and temperature ($T$) of the various components, are summarised in Table A-1. The validity range of $T$ is also provided.

**Table A-1: Summary of Antoine information for the various components.**

| Component | $A_k$ | B | C | Units of $P_i$ | Units of T | T validity range (˚C) |
|---|---|---|---|---|---|---|
| Water | 8.05573 | 1 723.64 | 233.076 | mmHg | ˚C | 0.01 – 373.98 |
| Ethanol | 5.24677 | 1 598.67 | -46.424 | Pa | K | 19.65 – 93.45 |
| Geraniol | 8.60515 | 2 773.11 | 254.443 | mmHg | ˚C | 4 – 230 |

The first assumption that was made is that the geraniol is completely immiscible with the water or ethanol at the end concentrations after the addition of additional water, but the water and ethanol are miscible. Therefore two phases existed: geraniol with the other phase being water and ethanol. The combined vapour pressure of the system can then be estimated by Raoult's Law shown in Equation 18.

$$P_{TOT} = P_G + P_{EW} \qquad (18)$$

Where: $P_G$ is the vapour pressure of the geraniol and $P_{EW}$ is the vapour pressure of the ethanol and water phase.

The vapour mole fractions of the respective phases (represented by $y_i$) can then be calculated by using Equation 19.

$$y_i P_{TOT} = P_i \tag{19}$$

The vapour pressure of the ethanol-water phase was also estimated with Raoult's law for non-ideal miscible liquids shown in Equation 20.

$$P_{EW} = \sum_0^i \gamma_i x_i P_i \tag{20}$$

Where: $\gamma_i$ is the activity coefficient and $x_i$ is the liquid phase mole fractions, respectively, of either ethanol or water within the ethanol-water phase.

The vapour mole fractions (by just considering the ethanol-water phase) were then calculated using Equation 21.

$$y_i P_{EW} = \gamma_i x_i P_i \tag{21}$$

The activity coefficients were calculated using the Margules Equation given by Equation 22.

$$\mathrm{Ln}(\gamma_i) = x_j^2 [A_{ij} + 2(A_{ji} - A_{ij}) x_i] \tag{22}$$

Where: $A_{ij}$ and $A_{ji}$ are factors dependent on temperature, but the temperature dependency was ignored in this study.

The mass loss recorded in the TGA analysis were reasonably assumed to be only that of water, ethanol and geraniol, i.e. zein did not contribute. Therefore, by combining the vapour mole fractions of the two phases from Equation 19 and the subsequent vapour mole fractions from Equation 21, the composition of the mass loss recorded in the TGA analysis could be estimated. With each measurement taken, the mass loss of each component could be calculated, and by simple mass balance the composition of the liquid remaining could be estimated. The initial compositions of the ethanol-water liquid phase and the total liquid system were initially unknown and therefore reasonably guessed. This guess was corrected by iteration until an error of less than 2% was achieved. Points of importance are:

- By applying Equations 18 to 21, the system is assumed to be closed and to be at equilibrium with each measurement, which is definitely not the case. However, for the approximations calculated, the estimates proved sufficient.
- Note that the ethanol-water liquid phase would not have reached an azeotrope at this composition or at a higher water composition (as the ethanol is evaporated at a higher rate). If the captured vapour were cooled repeatedly then the azeotrope would have been reached as the ethanol content of the vapour would increase.
- The overall two-phase system also did not reach a heterogenic azeotrope as the initial ethanol and water mole fraction in the entire liquid system was lower than the azeotropic composition, even in the case of the highest possible initial compositions (see Figure A-1).

At the bubble point of the binary system, the total vapour pressure will equal the absolute pressure which was held constant at 1.1 bar. Therefore $P_{TOT}$ at the bubble point can be equated to $P_{abs}$. From this the bubble point temperature can be calculated, which in this case was a range as $P_{TOT}$ is a function of the respective ethanol and water content in the ethanol-water phase which shifts until only pure water is left. Consequently the vapour phase mole fractions at the bubble point at which the azeotrope would exist could be estimated with Equation 23.

$$y_i = P_i / (P_i + P_j) \qquad (23)$$

The range of bubble point temperatures and the corresponding ethanol-water vapour mole fractions calculated are shown in Table A-2.

**Table A-2: Calculated bubble point temperatures of the geraniol and ethanol-water immiscible binary system with azeotropic vapour mole fractions of the ethanol-water phase.**

| Actual temperature (˚C) | Saturation temperature (˚C) | Ethanol-water phase azeotropic vapour mole fraction | Actual ethanol-water phase liquid mole fraction |
|---|---|---|---|
| Geraniol-to-zein 2:1 system | | | |
| 30 | 95.2 | 0.994 | 0.878 |
| 50 | 96.7 | 0.994 | 0.858 |
| 100 | 102.1 | 0.992 | 0.386 |

Firstly from Table A-2, it can be seen that the changing composition of the ethanol-water phase has a significant effect on the bubble point temperature of the entire system. Similarly, although to a very small extent, the diminishing ethanol content causes the azeotropic mole fraction to decrease somewhat. What is of the real concern is that the initial liquid mole fraction of the ethanol-water phase is in all cases less than that of the azeotropic mole fraction. This leads to the composition of the remaining liquid to increase in geraniol content. Conclusively, and put in simple terms, the initial conditions were on the preferred side of the azeotrope. Figure A-1 shows the composition loci based on these calculations for the geraniol-to-zein 2:1 system.

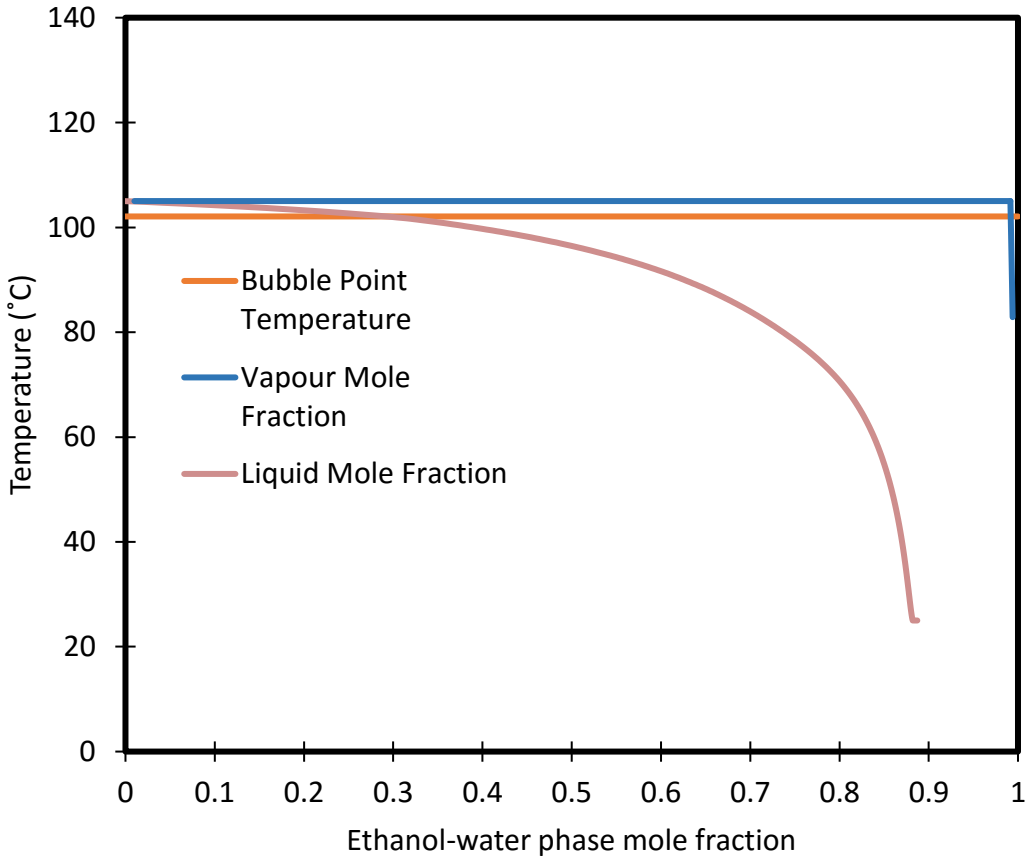


**Figure A-1: Composition loci of the immiscible geraniol and ethanol-water binary system.**

Note that the azeotropic mole fraction is extremely close to an ethanol-water phase only. This is due to the very great difference in volatility between geraniol and water/ethanol. Furthermore, the bubble point temperature of the system approaches that of water (102.3 ˚C at 1.1 bar) compared to that of geraniol (233˚C at 1.1 bar), indicating that initially very little geraniol is lost and that the initial mass loss is almost entirely due to ethanol and/or water as shown in Figure A-1. The water and ethanol should then be almost completely boiled off by 135 ˚C. This corresponds to the distinct peaks obtained in the experimental runs.